INDC(CCP)-1E

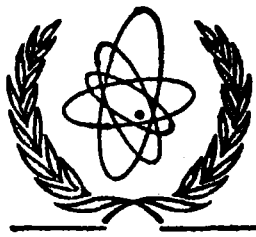

International Atomic Energy Agency

INDC-232
ENGLISH

USSR STATE COMMITTEE ON THE UTILIZATION OF ATOMIC ENERGY

NUCLEAR DATA INFORMATION CENTRE

Nuclear Physics Research in the USSR

(Collected Abstracts)

Issue 5, 1967

Obninsk 1967

68-4370

NUCLEAR PHYSICS RESEARCH IN THE USSR

COLLECTED ABSTRACTS

Issue 5

Atomizdat, 1967

English translation edited by A. Lorenz,
Nuclear Data Unit.

Institute of Physics and Power Engineering

LEVEL DENSITY OF ATOMIC NUCLEI

Yu. M. Shubin

(Article submitted to the bulletin of the Information Centre)

The author presents values of the level density parameter a calculated with the help of a semi-empirical formula obtained on the basis of experimental neutron resonance density data and taking into account the grouping of degenerate single-particle levels into shells. The calculations were performed for nuclei in the mass number range from Ne to Cm and for different proton:neutron ratios. The range of variations in the proton:neutron ratio was selected so as to cover the entire region from neutron-deficient nuclei obtained in reactions of the type (p, n), (d, n) etc., to neutron-rich nuclei with a neutron excess of the order of 20 (fission fragments).

INFLUENCE OF THE DEGENERATION OF SINGLE-PARTICLE LEVELS ON NUCLEAR STATE DENSITIES

Yu. M. Shubin

(Article submitted to "Jadernaja fizika")

The author discusses the influence of the detailed structure of the single-particle spectrum of a shell model on the nuclear state density. On the basis of results obtained using a simple model of equidistant single-particle levels with the same degeneration density, the author calculates quantitatively the influence of the extent to which the Fermi level is filled on the nuclear state density (Rosenzweig effect). In the selection of the model parameters account is taken of the grouping of degenerate single-particle levels into shells (Proceedings of Conference on Nuclear Data for Reactors, Paris, 17-21 October 1966). It is shown that allowance for the Rosenzweig effect substantially improves the agreement between theory and the experimental values of the level density parameter a.

The results of the calculations performed for light and intermediate nuclei indicate that the splitting of a level with given j, caused by a residual interaction, is significantly less than the average distance between the degenerate single-particle levels of the shell model.

INFLUENCE OF THE SHELL STRUCTURE OF FRAGMENTS ON THE FISSION PROCESS

A.V. Ignatyuk

(Article submitted to "Jadernajafizika")

Using a model with non-interacting particles moving in a deformed potential, the author studies the influence of shell structure on the deformation of fission products. The potential energy of the fissioning nucleus before scission is calculated in order to determine the fission fragment yield. It is shown that the minimum energy corresponds to assymetric fission for heavy fissioning nuclei and to symmetric fission for light nuclei. The calculated Coulomb energy of the deformed fragments at the point of scission explains the experimental values for the distribution of mean kinetic energies of the fragments as a function of fragment mass. The author calculates the most probable charge on fragments with a given mass.

Entered already as preprint by FD 68/Mar/17. PK

CROSS-SECTION RATIOS FOR ^{233}U, ^{235}U AND ^{239}U FISSION BY FAST NEUTRONS

G.N. Smirenkin and V.G. Nesterov

(Article submitted to the bulletin of the Information Centre)

Data are presented on cross-section ratios for ^{233}U, ^{235}U and ^{239}U fission by neutrons with energies in the range 0.3-2.5 MeV. The data were obtained in a single experiment using an ionization chamber and the glass detector technique. The measurements were accurate to within 3%. The results of this work are compared with those obtained by other authors.

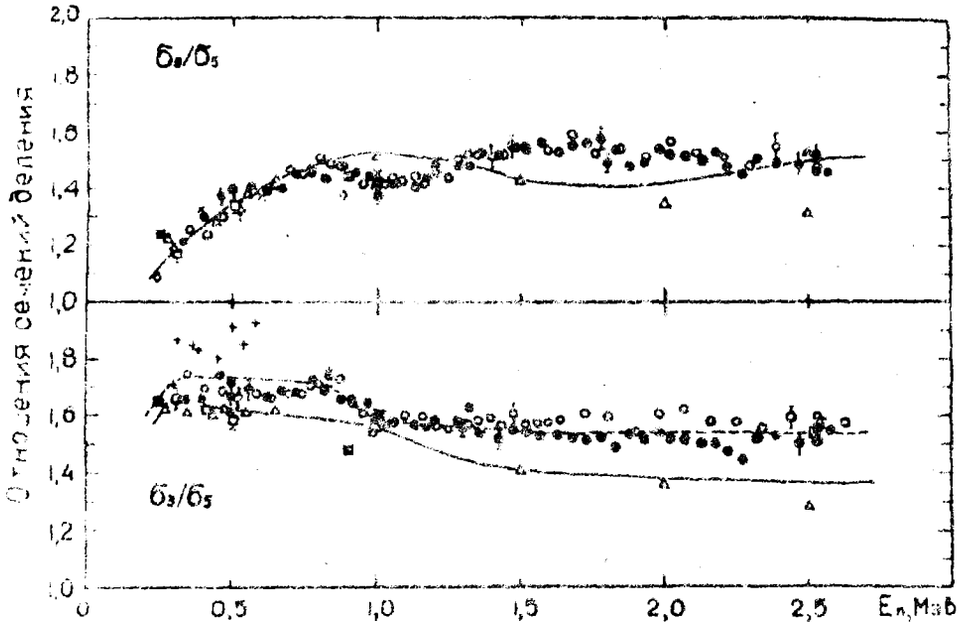

Fig. 1. Energy dependence of the cross-section ratios σ_3/σ_5 and σ_9/σ_5 for fission by neutrons with energies E_n = 0.3-2.5 MeV.

Δ – Allen, Ferguson;

▲ – Smith, Heukel, Nobles;

□ – White, Hodgkinson, Wall;

X – Dubrovina, Shigin;

\+ – Gorlov et al.;

▰ – Dorofeev et al.;

◆ – Andreev et al.;

O – Smirenkin et al.;

●,0 – data presented in the present work (● – ionization chamber, 0 – glass detector technique).

AVERAGE NUMBER OF PROMPT NEUTRONS IN ^{235}U AND ^{232}Th FISSION BY NEUTRONS WITH ENERGIES UP TO 3.3 MeV

L.I. Prokhorova and G.N. Smirenkin

The authors publish the results of relative measurements of the average number of prompt neutrons $\bar{\upsilon}$ in ^{232}Th fission by neutrons with energies ranging from 1.5 MeV to 3.3 MeV and ^{235}U fission by neutrons with energies ranging from 0.4 MeV to 3.3 MeV (in energy increments of 0.2 MeV). A battery of thirty-six $^{10}BF_3$ counters was used to measure $\bar{\upsilon}$. The fission events were recorded by means of a multilayer ionization chamber. The values for $\bar{\upsilon}$ were accurate to within about 1.5% for ^{235}U and about 2.5% for ^{232}Th. Measurements of $\bar{\upsilon}$ were performed by comparison with $\bar{\upsilon}$ ^{235}U for thermal neutrons.

Neutron energy, E_n	$\bar{\upsilon}$
	^{235}U
0.37 ± 0.10	2.474 ± 0.017
0.59 ± 0.10	2.471 ± 0.035
0.81 ± 0.09	2.461 ± 0.035
1.02 ± 0.08	2.538 ± 0.027
1.23 ± 0.08	2.556 ± 0.037
1.44 ± 0.07	2.564 ± 0.037
1.64 ± 0.07	2.589 ± 0.036
1.85 ± 0.07	2.619 ± 0.034
2.05 ± 0.06	2.607 ± 0.031
2.25 ± 0.06	2.678 ± 0.037
2.46 ± 0.06	2.760 ± 0.042
2.76 ± 0.06	2.816 ± 0.038
3.06 ± 0.05	2.825 ± 0.050
3.25 ± 0.05	2.852 ± 0.046

Neutron energy, E_n	$\bar{\upsilon}$
^{232}Th	
1.48 ± 0.03	2.179 ± 0.096
1.56 ± 0.05	2.096 ± 0.073
1.64 ± 0.07	2.132 ± 0.072
2.05 ± 0.06	2.142 ± 0.069
2.46 ± 0.06	2.221 ± 0.052
2.86 ± 0.05	2.213 ± 0.054
3.27 ± 0.04	2.416 ± 0.074

Preliminary results were presented by the authors at the Congrès International de Physique Nucléaire, Paris, July 1964 (paper 4 e/C336, I.I. Bondarenko et al.) and in the proceedings of the Conference on Nuclear Data for Reactors, Paris, 17-21 October 1966.

^{235}U FISSION BY NEUTRONS GIVING RISE TO A COMPOUND NUCLEUS WITH AN EXCITATION ENERGY OF 22 MeV

P.P. Dyachenko and B.D. Kuzminov

(Article submitted to "Jaderna ja fizika")

The authors report the results of a study of the energy and mass distributions of particles produced in ^{235}U fission by 15.5-MeV neutrons. The results are analysed for the purpose of isolating the fission fragment distribution corresponding to the excitation energy of the fissioning ^{236}U nucleus (~ 22 MeV). The authors discuss the change in the energy and mass distributions of the fission fragments as the excitation energy of the fissioning nucleus increases. It is noted that the energy distributions of the fission fragments change only slightly as the excitation energy increases from ~ 6 MeV to ~ 12 MeV, whereas there is a substantial change in the energy distributions of the fission fragments as the excitation energy increases from ~ 12 MeV to ~ 22 MeV, apparently due to a substantial decline in the influence of shell changes on the fission process in this excitation energy range.

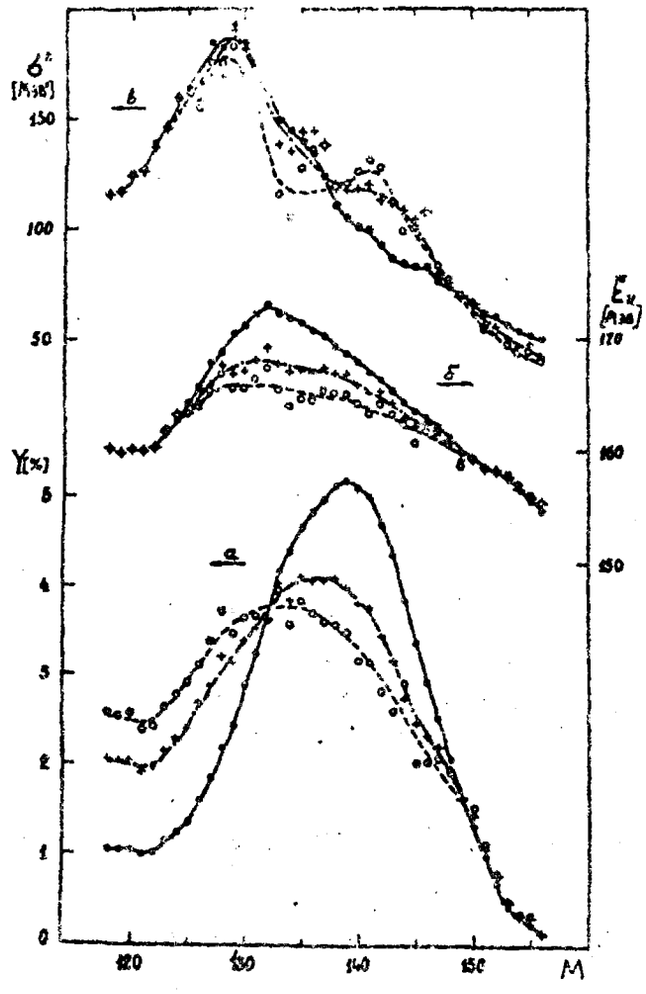

Fig. 1. Fission fragment yields as a function of mass (a), fission fragment kinetic energies as a function of mass (b), and mean square deviations of fission fragment kinetic energy as a function of mass (c) in ^{235}U fission by 15.5-MeV neutrons.

——— ● - measured distributions; —— 0 - results of analysis using partial cross-sections σ_{f0} = 1.0 barn, σ_{f1} = 0.86 barn, σ_{f2} = 0.60 barn, -.-.-. + - results of analysis using partial cross-sections σ_{f0} = 1.2 barn, σ_{f1} = 0.7 barn, σ_{f2} = 0.47 barn.

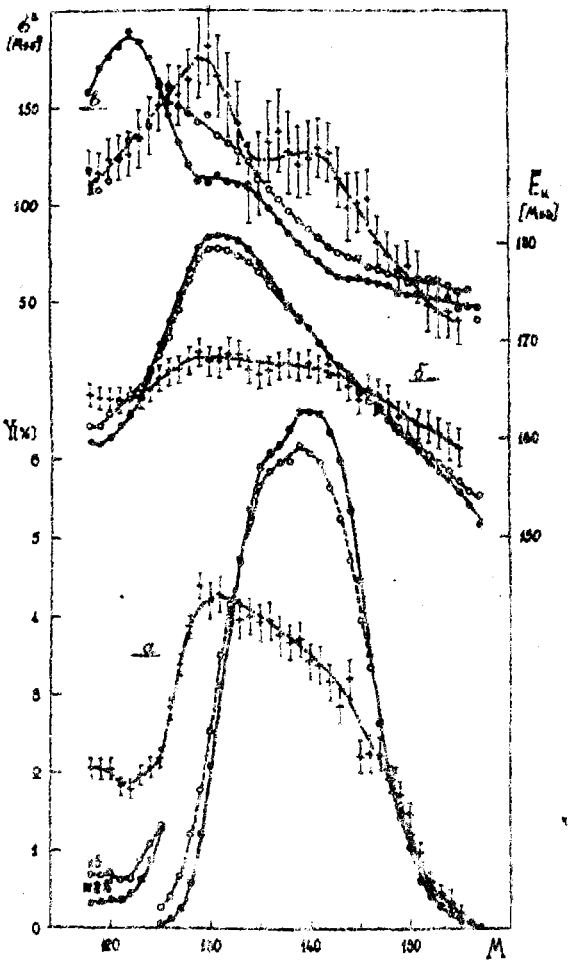

Fig.2. Fission fragment yields as a function of mass (a), fission fragment kinetic energies as a function of mass (b), and mean square deviations of fission fragment kinetic energy as a function of mass (c) for different excitation energies of the ^{236}U fissioning compound nucleus.

——●— 6.5 MeV; - - - - o - 12.5 MeV; -.-.-+-.- 22 MeV.

INFLUENCE OF TRANSITIONAL STATES OF THE FISSIONING ^{232}Th NUCLEUS ON THE MASS AND KINETIC ENERGY DISTRIBUTIONS OF THE FISSION FRAGMENTS

A.I. Sergachev, V.G. Vorobyeva, B.D. Kuzminov, V.B. Mikhailov and M.Z. Tarasko

The authors have investigated the mass and kinetic energy distributions of the fragments produced in ^{232}Th fission by neutrons with energies of 1.38, 1.51, 1.65, 1.9, 2.37, 2.87 and 5.6 MeV. Two surface-barrier counters were used to record the energies of the fission fragment ε_L and ε_H. The fission fragment masses were determined by means of the relation

$$\mu_H = \frac{\varepsilon_L}{\varepsilon_L + \varepsilon_H}$$

The final results were corrected for neutron emission by the fission fragments. Fragments produced in ^{235}U fission by thermal neutrons were used for calibration, allowance being made for the dependence of pulse amplitude on fission fragment mass. The main results are presented in the table and figures. As the neutron energies increase from 1.5 MeV to 1.65 MeV the mass and kinetic energy distributions of the fission fragments underwent marked changes. At E_n = 2.86 MeV there was a substantial increase in the yield of symmetrical fragments. The observed effects are attributed to the influence of transitional states of the fissioning nucleus. It is noted that the difference between nucleon configurations for fission through different channels may affect the form of the nucleus at the moment of break-up, causing a change in the fission fragment yields and kinetic energies.

INFLUENCE OF TRANSITIONAL STATES OF THE FISSIONING ^{232}Th NUCLEUS ON THE MASS AND KINETIC ENERGY DISTRIBUTIONS OF THE FISSION FRAGMENTS

A.I. Sergachev, V.G. Vorobyeva, B.D. Kuzminov, V.E. Mikhailov and M.Z. Tarasko

The authors have investigated the mass and kinetic energy distributions of the fragments produced in ^{232}Th fission by neutrons with energies of 1.38, 1.51, 1.65, 1.9, 2.37, 2.87 and 5.6 MeV. Two surface-barrier counters were used to record the energies of the fission fragment ε_L and ε_H. The fission fragment masses were determined by means of the relation

$$\mu_H = \frac{\varepsilon_L}{\varepsilon_L + \varepsilon_H}$$

The final results were corrected for neutron emission by the fission fragments. Fragments produced in ^{235}U fission by thermal neutrons were used for calibration, allowance being made for the dependence of pulse amplitude on fission fragment mass. The main results are presented in the table and figures. As the neutron energies increase from 1.5 MeV to 1.65 MeV the mass and kinetic energy distributions of the fission fragments underwent marked changes. At E_n = 2.86 MeV there was a substantial increase in the yield of symmetrical fragments. The observed effects are attributed to the influence of transitional states of the fissioning nucleus. It is noted that the difference between nucleon configurations for fission through different channels may affect the form of the nucleus at the moment of break-up, causing a change in the fission fragment yields and kinetic energies.

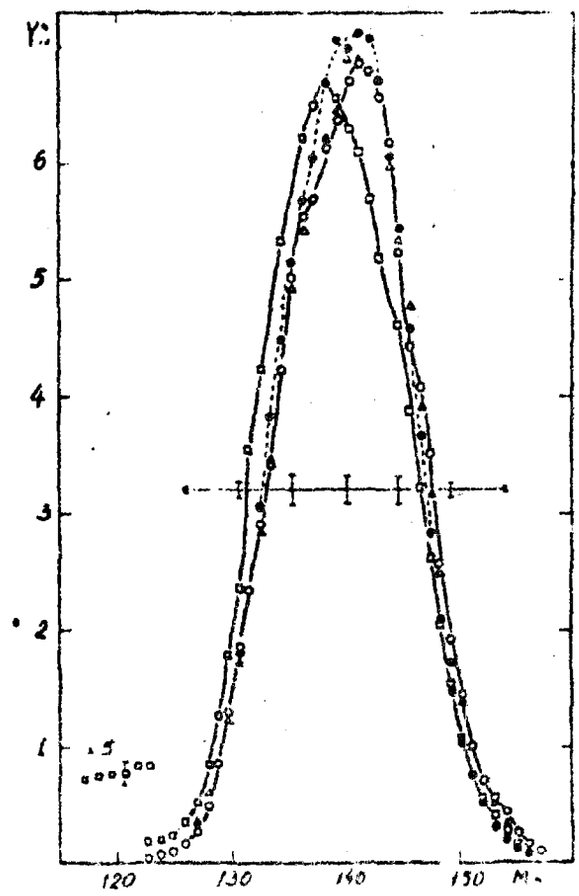

Fig. 1 Mass distribution of fission fragments for ^{232}Th fission by neutrons with energies of 1.38 MeV (o), 1.51 MeV (Δ), 1.65 MeV (●), 5.6 MeV (□).

E_n	$^{+0.020}$	$^{+0.090}$	$^{+0.100}$	$^{+0.100}$	$^{+0.130}$	$^{+0.130}$	$^{+0.200}$
MeV	1.38	1.510	1.650	1.900	2.370	2.870	5.600
	$^{-0.120}$	$^{-0.130}$	$^{-0.130}$	$^{-0.150}$	$^{-0.180}$	$^{-0.200}$	$^{-0.200}$
E_k							
MeV	161.45 ± 0.22	161.20 ± 0.18	162.73 ± 0.16	162.55 ± 0.16	163.17 ± 0.16	163.02 ± 0.16	163.47 ± 0.18

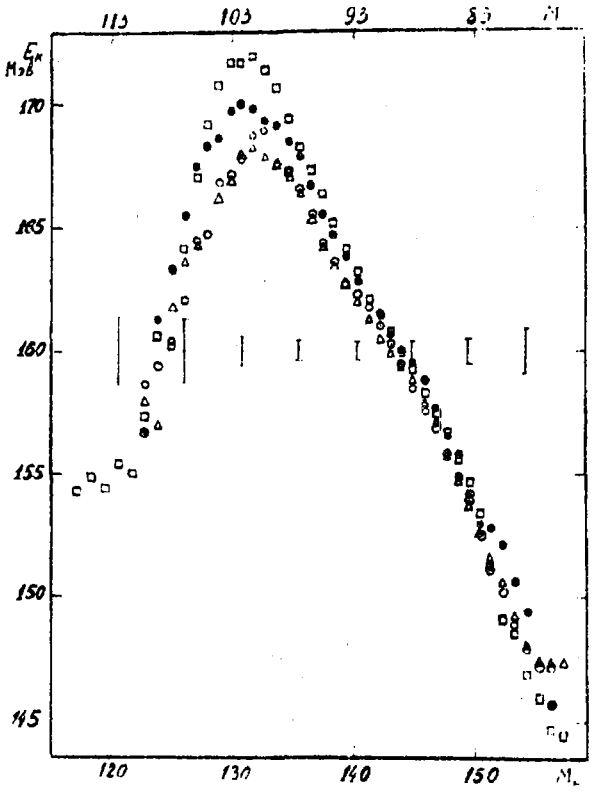

Fig. 2. Mass dependence of the kinetic energy of fragments produced in ^{232}Th fission by neutrons with energies of 1.38 MeV (o), 1.51 MeV (Δ), 1.65 MeV (●), 5.6 MeV (□).

RELATIVE YIELDS OF DELAYED NEUTRONS IN ^{235}U FISSION BY NEUTRONS WITH ENERGIES OF 18–21 MeV

B.P. Maksyutenko, R. Ramazanov and M.Z. Tarasko

The authors have measured the relative yields of delayed neutrons in ^{235}U fission by neutrons with energies of 18.0, 19.0, 19.7, 20.3 and 20.5 MeV. The experiment was performed in a Van de Graaff accelerator using a tritium-zirconium target with a thickness of 15 mg/cm^2. The decay curve calculations were performed on a computer. The results are presented in Table 1.

TABLE 1

$T_{\frac{1}{2}}$ Sec	Ratio of Yields
	E_n = 18.0 MeV
55	I
24	2.153 + 0.060
15.5	1.874 + 0.085
5.2	3.11 + 0.13
2.2	6.94 + 0.27
	E_n = 19.0 MeV
55	I
24	2.703 + 0.092
15.5	1.55 + 0.12
5.2	3.86 + 0.19
2.2	6.02 + 0.38
	E_n = 19.7 MeV
55	I
24	2.816 + 0.076
15.5	1.94 + 0.11
5.2	3.208 + 0.063
2.2	7.349 + 0.033
	E_n = 20.3 MeV
55	I
24	2.702 + 0.096
15.5	2.24 + 0.13
5.2	2.562 + 0.037
2.2	10.24 + 0.42
	E_n = 20.5 MeV
55	I
24	3.116 + 0.087
15.5	1.655 + 0.080
5.2	3.69 + 0.14
2.2	6.02 + 0.27

RADIATIVE CAPTURE OF FAST NEUTRONS BY ^{80}SE

V.A. Tolstikov, V.P. Koroleva and V.E. Kolesov

Using the activation method, the authors have measured cross-sections for the radiative capture of fast neutrons in ^{80}Se and for the reactions ^{80}Se (n,γ) ^{81m}Se and ^{80}Se (n,γ) ^{81g}Se. The total radiative capture cross-section is compared with calculated values obtained on the basis of the statistical theory of nuclear reactions using the optical model. The isomeric ratio is constructed on the basis of the experimental data.

Table I

Cross-sections for the radiative capture of fast neutrons by ^{80}Se

E_n (keV)	200	266	338	456	635	679	741	777	
$\sigma(n,\gamma)$, (mbarn)	15.9±1.7	13.8±1.8	12.5±1.1	11.8±1.1	9.8±0.8	7.9±0.75	6.3±0.6	6.3±0.6	
E_n (keV)	844	920	1024	1335	1523	1690	1917	2323	3128
$\sigma(n,\gamma)$, (mbarn)	5.25±0.55	4.8±0.4	4.4±0.4	4.3±0.4	3.4±0.4	2.9±0.3	3.1±0.3	2.75±0.4	2.3±0.2

CROSS-SECTIONS FOR THE RADIATIVE CAPTURE OF FAST NEUTRONS BY ^{74}Ge, ^{133}Cs AND ^{192}Os

V.A. Tolstikov, V.P. Koroleva
V.E. Kolesov and A.G. Dovtenko

(Article submitted to "Atomnaja energija")

The authors present the results of measurements of cross-sections for the radiative capture of neutrons with energies of 0.3-3 MeV by ^{74}Ge, ^{113}Cs and ^{192}Os. The neutron capture events were recorded by the activation method. A fission chamber containing ^{235}U was used as neutron flux monitor. The measured cross-sections are compared with values calculated on the basis of statistical theory using the optical model for calculating the penetrability of potential nuclear barriers.

The experimental results are presented in Tables I-III.

TABLE I

Cross-sections for the radiative capture of fast neutrons by ^{74}Ge

En keV	200 ± 30	242 ± 35	338 ± 37	394 ± 60	433 ± 60	515 ± 58	612 ± 56	688 ± 55
σn,γ mb	17.0 ± 1.3	14.8 ± 1.1	13.0 ± 0.7	15.0 ± 0.7	15.1 ± 1.2	13.3 ± 1.3	11.9 ± 0.7	8.7 ± 0.7
En keV	720 ± 54	777 ± 54	824 ± 53	929 ± 52	1034 ± 51	1240 ± 48	1523 ± 75	1690 ± 74
σn,γ mb	8.8 ± 0.4	8.0 ± 0.7	8.1 ± 0.6	6.9 ± 0.35	6.5 ± 0.3	5.6 ± 0.4	4.1 ± 0.2	3.8 ± 0.2
En keV	1857 ± 74	1917 ± 7.3	2120 ± 71	2186 ± 71	2323 ± 69	2723 ± 66	31.8 ± 65	
σn,γ mb	4.25 ± 0.3	4.5 ± 0.3	6.6 ± 0.3	4.5 ± 0.3	4.7 ± 0.3	4.74 ± 0.3	4.0 ± 0.3	

TABLE II

Cross-sections for formation of the isomer ^{134m}Cs in the reaction $^{133}Cs(n,\gamma)$ ^{134m}Cs

En keV	142 ± 50	274 ± 62	418 ± 60	500 ± 58	593 ± 60	814 ± 62
σn,γ mb	36.0 ± 3	29.2 ± 2	26.1 ± 2.7	25.8 ± 1.8	24.5 ± 1.7	19.1 ± 1.6
En keV	950 ± 60	1230 ± 57				
σn,γ mb	19.4 ± 1.7	17.9 ± 1.3				

T A B L E III

Cross-sections for the radiative capture of fast neutrons by ^{192}Os

En keV	200 ± 35	338 ± 37	423 ± 40	433 ± 45	505 ± 50	600 ± 56	824 ± 53	960 ± 50
σn,γ mb	49.9 ± 3.6	33.7 ± 1.9	23.7 ± 1.7	23.4 ± 1.2	284 ± 1.2	20.1 ± 1.0	18.3 ± 0.9	18.4 ± 1.3
En keV	1140 ± 50	1240 ± 50	1440 ± 48	1690 ± 50	1857 ± 60	1917 ± 73	2120 ± 71	2320 ± 69
σn,γ mb	15.9 ± 1.4	17.1 ± 1.0	16.0 ± 1.3	16.7 ± 1.3	15.2 ± 1.0	15.7 ± 1.1	14.9 ± 1.0	12.7 ± 0.8
En keV	2517 ± 68	2624 ± 66	3130 ± 65					
σn,γ mb	12.55 ± 1.00	10.4 ± 0.7	8.3 ± 0.5					

RELATIVE PROBABILITIES OF ISOMERIC STATE EXCITATION IN THE RADIATIVE CAPTURE OF THERMAL NEUTRONS

A.V. Malyshev

(Article submitted to "Jadernaja fizika")

The relative probabilities of isomeric state formation in the radiative capture of thermal neutrons are calculated on the basis of statistical theory. In order to verify the dependence of nuclear level density on total nuclear momentum the author takes into account the distribution of gamma sources in each cascade. Taking as his example eight odd-odd nuclei for which the isomeric ratios differ by a factor of ~30 the author shows that, if the sole parameter of the theory (the density of single-particle states near the Fermi energy) is given, agreement is obtained with experiment to within 50%.

THE REACTIONS Li + $^{4}_{2}$He, Li + $^{2}_{1}$He AND Li + $^{1}_{1}$He AS CYCLOTRON SOURCES OF FAST NEUTRONS

V.K. Daruga, V.G. Dvukhsherstnov, V.A. Dulin,
N.N. Krasnov and E.S. Matusevich

(Article submitted to the bulletin of the Information Centre)

The authors have studied the yields and the energy and angular distributions of fast neutrons ($E_n \geq 1$ MeV) from a thick Li target (natural isotopic mixture) bombarded with helium ions, deuterons and protons with energies of 42 ± 1 MeV, 20 ± 0.5 MeV and 21 ± 0.5 MeV respectively. The 1.5-m cyclotron of the Institute of Physics and Power Engineering was used for accelerating the charged particles.

The energy spectra of the neutrons were measured at ~0° and 90° to a beam of charged particles in the energy range 1-18 MeV by means of a single-crystal scintillation fast-neutron spectrometer with gamma-ray discrimination by de-excitation time. Angular distributions within the range 0-140° were measured by means of the laboratory ZnS (Ag) fast-neutron detector.

Data on fast neutron yields from an Li target are presented in Table I.

Table I

Particle	Particle energy (MeV)	Neutron yield at ~0° to beam per 1 μC, steradian		Total neutron yield per 1 μC
$^{4}_{2}He$	42 ± 1	$6.9.10^{9}$ ± 14%		-
$^{2}_{1}H$	20 ± 0.5	$6.2.10^{10}$ ± 13%	$E_n > 1$ MeV	-
$^{1}_{1}H$	21 ± 0.5	$4.2.10^{9}$ ± 10%		-
		$7.6.10^{9}$ ± 15%	$E_n > 0$	$4.9.10^{10}$ ± 18%

EXCITATION FUNCTION OF THE REACTION ^{65}Cu (p,n) ^{65}Zn

P.P. Dmitriev, I.O. Konstantinov and N.N. Krasnov

(Article submitted to "Atomnaja energija")

Using the cyclotron of the Institute of Physics and Power Engineering and the foil stack method, the authors have measured the excitation function of the reaction ^{65}Cu (p,n) ^{65}Zn for proton energies up to E_p = 22 MeV. By integrating the excitation function over the path length they have obtained a curve showing the ^{65}Zn yield for a thick copper target. The results are compared with the data of other authors and with calculations based on the statistical model.

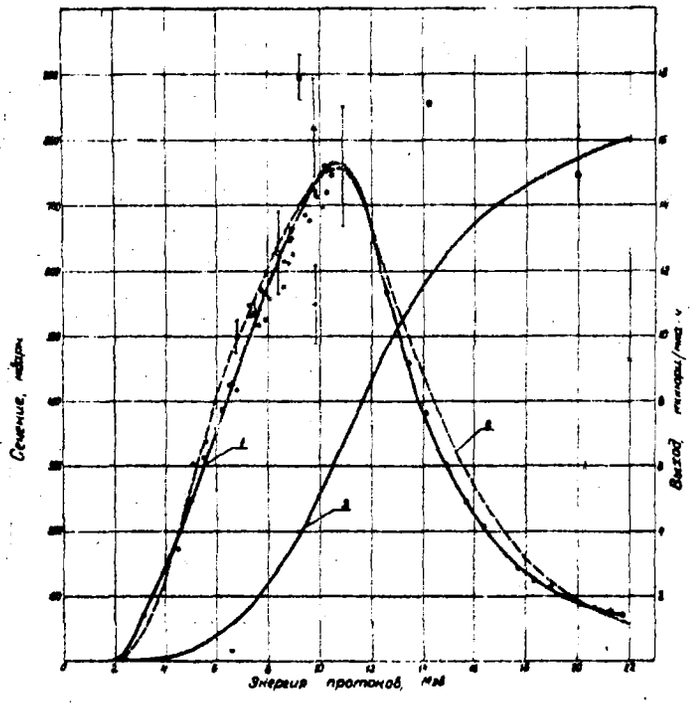

Fig. 1 Comparison of results of present work (●) with measurements made by other authors:

1 - Experimental excitation function;

2 - Calculated excitation function for $r_0 = 1.6$ f;

3 - Dependence of ^{65}Zn yield on proton energy.

Table 1

Experimental values of the cross-section for the reaction $^{63}Cu\ (p,n)\ ^{65}Zn$

Deuteron energy (MeV)	Reaction cross-section (mbarn)
22.8	71
21.2	[illegible]
20.7	82
[illegible]	[illegible]
19.6	100
[illegible]	[illegible]
[illegible]	12
17.7	[illegible]
[illegible]	17
[illegible]	20?

Deuteron energy (MeV)	Reaction cross-section (mbarn)
15.7	248
14.9	301
14.2	382
13.4	460
12.6	566
11.8	702
10.9	759
10.0	750
9.0	665
7.9	566
6.6	430
5.0	250
3.2	74

INELASTIC NEUTRON SCATTERING

V.M. Sluchevskaya

(article submitted to the bulletin
of the Information Centre)

The author presents experimental data published before July 1967 on the following:

(a) Inelastic scattering cross-sections;

(b) Cross-sections for level excitation in inelastic scattering;

(c) Cross-sections for gamma emission in inelastic scattering; and

(d) Angular distributions of inelastically scattered neutrons and gamma rays.

The paper also includes group cross-sections (recommended on the basis of an analysis of experimental data) for the inelastic scattering of neutrons in certain elements employed in reactor construction.

CROSS-SECTION FOR THE (n, 2n) REACTION

V.N. Shuchevskaya

(article submitted to the bulletin of the Information Centre)

The author presents data published before July 1967 on the measurement of cross-sections for the (n, 2n) reaction.

SPECTRA OF SECONDARY NEUTRONS IN THE (n, 2n) REACTION

Yu.N. Shubin

On the basis of the statistical theory of nuclear reactions, the author has calculated the spectra of secondary neutrons in the (n, 2n) reaction for incident neutron energies of 14 MeV. Comparison of these calculations with the results presented in [1] has shown that the discrete structure of the spectrum of the low-lying excited levels of the residual nucleus has a determining effect on the relative energy distribution of secondary particles. From this it may be deduced that, even when the residual nucleus has a large number of levels, transitions to separate levels are the basic pattern, due to angular momentum selection. Neutrons with an energy of 14 MeV introduce a large orbital momentum (~ 10). At the same time, inelastically scattered neutrons have a Maxwellian spectrum with a mean energy of about 1 MeV - **i.e.** they carry off only a little momentum (1-2). Secondary neutrons also carry off relatively little momentum, so that the residual nucleus necessarily retains considerable momentum. Fig. 1 shows the results of calculations of the spectrum of secondary neutrons for transitions to the ground state and the first excited state of the ^{47}Ti nucleus. These states have **fairly** high spins [2] of 5/2 and 7/2 respectively. It may be concluded from a comparison of the calculated results with the experimental spectrum that, in the case in question, transition is basically to the first excited level (E_2 = 0.2 MeV), which has a higher spin (7/2) than the ground state (5/2). It should be noted that the shape of the spectrum is fairly sensitive to the structure of the spectrum of the low-lying excited levels, so that a shift of 0.2 MeV in the energy of the E_2 level leads to a spectrum shape that differs markedly from the experimental shape.

The maximum energy of the secondary neutrons in the reaction ^{55}Mn (n, 2n) ^{54}Mn is about 2 MeV - i.e. in the case in question transitions occur not to the ground state of the ^{54}Mn nucleus (the maximum energy would then be 3.8 MeV [3]) but to a state having an energy of about 2 MeV (and not less than 1.8 MeV). One may therefore expect the ^{54}Mn nucleus to have, in the 2-MeV region, a level with high spin (~ 5.6) or a group of levels.

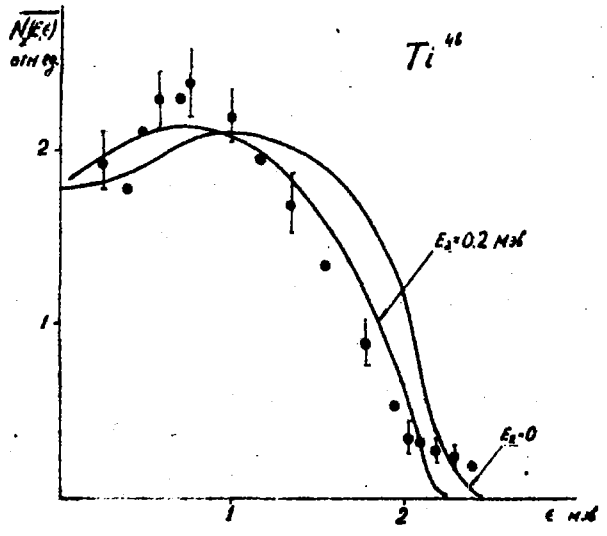

Fig. 1 Relative energy distribution of secondary neutrons in the reaction ^{48}Ti (n, 2n) ^{47}Ti for transition to a single isolated level (E_2 = 0 and E_2 = 0.2 MeV; continuous curves). The points with error bars denote the experimental distribution.

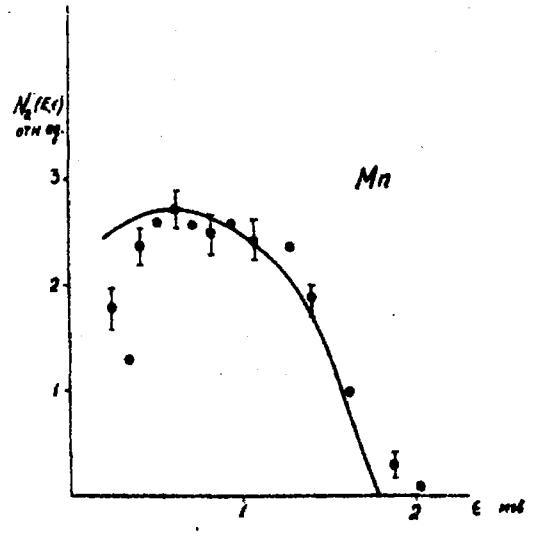

Fig. 2 Relative energy distribution of secondary neutrons in the reaction ^{55}Mn (n, 2n) ^{54}Mn for transition to a single level having an energy E_2 = 2 MeV (continuous curve). The points denote the experimental distribution.

In Fig. 2 the experimental spectrum is compared with calculations for transitions to the E_2 = 2 MeV level of the ^{54}Mn nucleus. The agreement between them is fairly good, except at low energies, owing possibly to the energy dependence of the cross-section for the reverse process, which is not taken into account in these calculations.

References

[1] V.B. Anufrienko et al., Jadernaja fizika 2 (1965) 826.

[2] B.S. Dzhelepov and L.K. Peker, Shemy raspada radioaktivnyh jader (Decay schemes of radioactive nuclei), (1966).

[3] J.H.E. Mattauch, W. Thiele and A.H. Wapstra, Nucl. Phys. 67 (1965) 1.

MONTE CARLO CALCULATIONS OF CORRECTIONS TO EXPERIMENTAL CROSS-SECTIONS FOR ELASTIC NEUTRON SCATTERING

V.I. Popov, V.M. Sluchevskaya and V.I. Trykova

The authors describe Monte Carlo programmes designed for correcting measured differential elastic scattering cross-sections for effects arising out of the finite sample and detector dimensions (neutron flux attenuation and multiple neutron scattering in samples, angular resolution of the sample-detector system). The programme is written in Algol-60.

ANISOTROPY OF ELASTIC NEUTRON SCATTERING

M.N. Nikolaev and N.O. Bazazyants

(article submitted to the bulletin of the Information Centre)

The authors present the energy dependencies of the Legendre polynomial expansion coefficients B_n of the angular distributions of elastically scattered neutrons:

$$\sigma_s(\mu, E) = \frac{1}{4\pi} \sum_{n=0}^{N} B_n (E) P_n (\mu)$$

The number N of terms in the expansion is chosen so as to ensure that the curve describing the experimental angular distribution data falls within the error limits.

The authors discuss methods of expansion coefficient determination that will ensure satisfactory description of the experimental data, the accepted way of introducing corrections for inelastic scattering, and other questions concerning the systematic processing of experimental data and the use of the information in performing calculations.

In the region of sufficiently high energies, where the contribution of inelastic scattering accompanied by the formation of a compound nucleus is small, the angular distributions of elastically scattered neutrons are calculated on the basis of the optical model.

Graphs are presented showing the energy dependencies B_n for 46 elements and isotopes. The upper limit of the energy region considered is 15 MeV.

The work also contains a short survey of the basic characteristics of the experimental methods used in measuring angular distributions; these characteristics are presented in a special table together with standard bibliographical data on the experimental works referred to (over 180).

Graphs showing the energy dependencies of the coefficients B_n are accompanied by a commentary containing a discussion of the adequacy of the available data, the compatibility of the data of different authors, and an analysis of the possible causes of discrepancies.

The authors give recommended energy dependencies of the Legendre polynomial expansion coefficients of the angular distributions of elastically scattered neutrons.

NUCLEAR PHYSICS CONSTANTS FOR REACTOR CALCULATIONS

S.M. Zakharova, G.I. Toshinsky and B.N. Sivak

(published in the bulletin of the Information Centre
(issue 3, supplement 1))

The authors present a 21-group set of nuclear physics constants compiled on the basis of experimental data on neutron-nucleus interaction cross-sections published before May 1966. The set is designed for reactor calculations on a computer and contains the following elements and isotopes:

H, ^{6}Li, ^{7}Li, Li, ^{9}Be, ^{10}B, ^{11}B, B, C, O, Al, Na, K, Ca, Ti, V, Cr, Fe, Ni, Cu, Y, Zr, Nb, Mo, Ta, W, Pb, Bi, ^{235}U, ^{236}U, ^{238}U, ^{239}Pu, ^{240}Pu, ^{241}Pu, ^{242}Pu and fission fragments of ^{235}U. For Mn, Co, ^{63}Cu, ^{65}Cu, Ga, ^{90}Zr, ^{91}Zr, ^{92}Zr, ^{94}Zr, ^{96}Zr, ^{92}Mo, ^{94}Mo, ^{95}Mo, ^{96}Mo, ^{97}Mo, ^{98}Mo, ^{100}Mo, ^{113}Cd, Cd, ^{115}In (54 min.), Sn, ^{135}Xe, ^{138}Ba, ^{147}Sm, ^{149}Sm, ^{150}Sm, ^{151}Sm, ^{152}Sm, Sm, ^{151}Eu, ^{153}Eu, Eu

and Hf only capture cross-sections are presented, while fission cross-sections are presented for ^{237}Np.

In addition to the 21-group set of constants, the authors have constructed 80-group radiative capture cross-sections for all the elements and isotopes listed above, as well as ν, α, fission cross-sections and total absorption cross-sections for the fissile isotopes. For some of the elements and isotopes listed, cross-sections for the (n, p) and (n, α) reactions are also presented.

As thermal group constants, the authors present, in addition to the cross-section values for 0.0253-eV neutrons, cross-sections - averaged over the Maxwellian spectrum as a function of neutron gas temperature and the point of thermal and slowing-down spectrum overlap (this relates to capture, fission and total absorption cross-sections) for

^{103}Rh, ^{113}Cd, ^{115}In, ^{123}Te, ^{135}Xe, ^{139}La, ^{149}Sm, ^{151}Sm, ^{151}Eu, ^{153}Eu, ^{155}Dy, ^{155}Gd, ^{157}Gd, ^{167}Er, ^{168}Yb, ^{176}Lu, ^{177}Hf, ^{182}Ta, ^{185}Re, ^{191}Ir, ^{193}Ir, ^{226}Ra, ^{233}U, ^{235}U, ^{239}Pu, ^{241}Pu, ^{242}Pu

and for a $1/\nu$ absorber. Finally, they present transport elastic cross-section values averaged over the Maxwellian spectrum for Be and H (in chemical compounds such as water and zirconium hydride).

Institute of Theoretical and Experimental Physics

LONG-RANGE PARTICLES WITH Z > 2 IN TERNARY ^{235}U FISSION BY THERMAL NEUTRONS

V.N. Andreev, V.G. Nedopekin and V.I. Rogov

The authors have studied the emission of particles with Z > 2 in ^{235}U fission by thermal neutrons. The particles were recorded by means of a detector which measured dE/dX, E and R for each particle. Lithium, beryllium, boron, carbon, nitrogen, oxygen and fluorine were detected. The ion energy spectra were measured and the isotopic composition of the ions assessed. There was found to be preferential emission of even Z ions and of even N isotopes. The measured ion yields, the minimum energy of the detected particles and the total ion yield estimated by extrapolating the experimental spectrum into the region of low-energy ions, are presented in the table below.

Ions	Yield per fission	E_{min} (MeV)	Total yield per fission
α-particles	2×10^{-3}	6	2.1×10^{-3}
lithium	$(1.33 \pm 0.08) \times 10^{-6}$	11	1.9×10^{-6}
beryllium	$(4.13 \pm 0.22) \times 10^{-6}$	15	6.8×10^{-6}
beryllium-8	$(5 \pm 2) \times 10^{-8}$	15	10^{-7}
boron	$(5.1 \pm 0.7) \times 10^{-8}$	20	10^{-7}
carbon	$(1.9 \pm 0.1) \times 10^{-6}$	29	1.0×10^{-5}
nitrogen	$(8.9 \pm 0.0) \times 10^{-8}$	33	5×10^{-7}
oxygen	$(6.1 \pm 1.2) \times 10^{-7}$	40	10^{-5}
fluorine	$(2.1 \pm 0.7) \times 10^{-8}$	47	5×10^{-6}

The spectra of the ions at the moment of their formation during fission are calculated from the experimental spectra. The spectra have the form $N(E_o) \sim e^{\frac{-E_o}{T}}$, where E_o is the initial ion energy calculated without allowing for the velocity along the fission axis and T is a parameter.

TOTAL NEUTRON CROSS-SECTION OF ^{230}Th IN THE THERMAL ENERGY REGION

S.M. Kalebin, P.N. Paley, R.N. Ivanov, Z.K. Karalova, G.M. Kukavadze, Z.I. Pyzhova and G.V. Rukolaine

For the investigation of the total neutron cross-section, 1 g of ^{230}Th is extracted chemically from uranium ore and purified. The purity of the sample is determined by mass spectrometry. The neutron cross-section measurements are made on the Institute's mechanical chopper in the energy range 0.0141-1.0 eV. As a result of the measurements it is established that the neutron cross-section of ^{230}Th in the thermal energy region is characterized by the presence of resonance levels close to this region. In particular, there is evidence of a negative level with energy close to zero. The measured total neutron cross-section of ^{230}Th at the thermal energy (E = 0.025 eV) is 70 ± 3.8 barn.

In measurements with a new thorium sample conducted over a wider energy range, levels with E = 0.107 eV, 2.390 eV and 7.80 eV have not been detected.

The results of the measurements are shown in the figure. Curve I represents the energy dependence of the total neutron cross-section of ^{230}Th. The crosses represent the result of an independent measurement of this cross-section using a single-channel time analyser. The measured total neutron cross-section of ^{232}Th, relative to which the ^{230}Th cross-section is measured, is represented by curve II. The circles indicate the ^{232}Th cross-section data taken from published works.

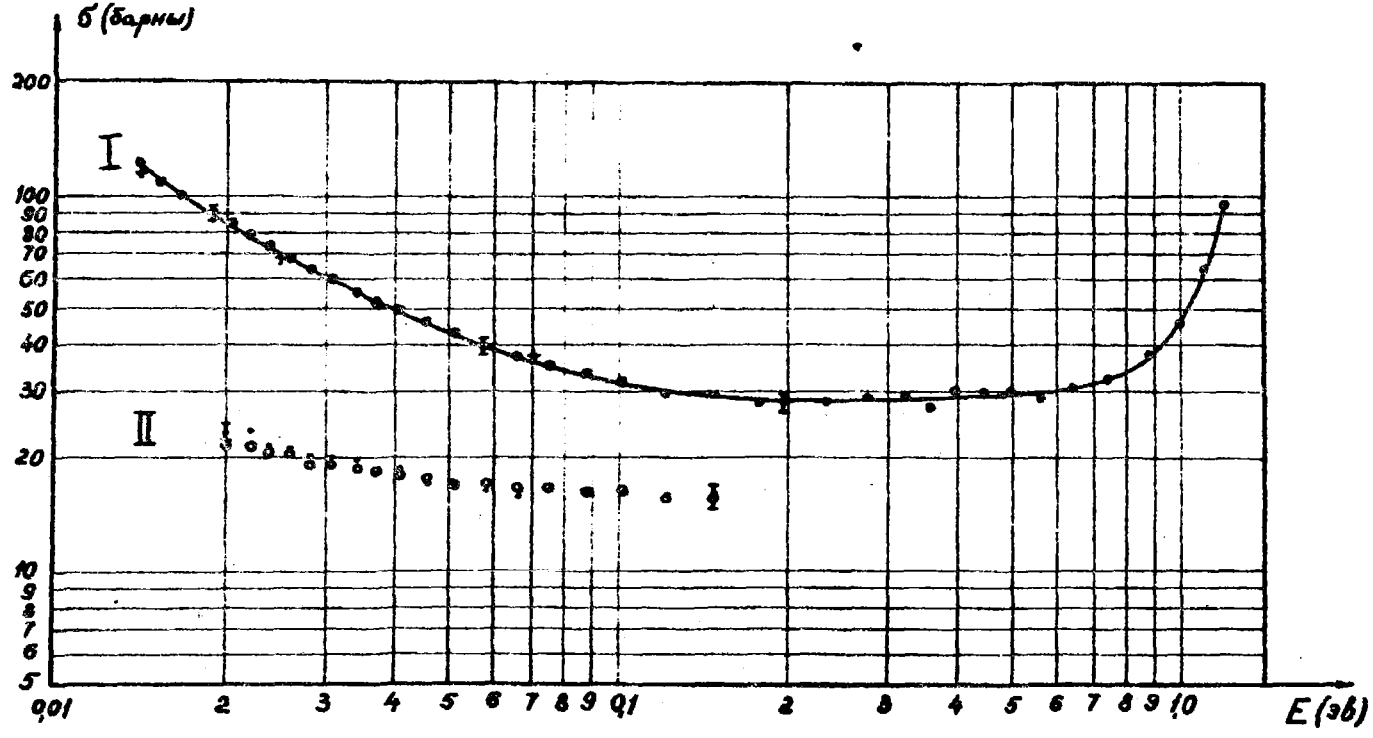
σ (барны)
200
100
90
80
70
60
50
40
30
20
10
9
8
7
6
5
I
II
0,01
2
3
4
5
6
7
8
9
0,1
2
3
4
5
6
7
8
9
1,0
E (эв)

A.F. Ioffe Institute of Physics and Technology,
USSR Academy of Sciences

MEASUREMENT OF THE REACTOR CROSS-SECTION FOR ^{46}Sc AND ^{64}Cu BURN-UP

I.A. Kondurov, A.I. Egorov, D.M. Kaminker,
E.M. Korotkikh and A.M. Nikitin

(article submitted to "Atomnaja energija")

The ^{46}Ti (n, p) ^{46}Sc reaction is a convenient means of monitoring fast neutrons. However, in high neutron fluxes ^{46}Sc may burn up due to neutron capture and thus lower the induced activity, which is a measure of the flux. The cross-section for ^{46}Sc burn-up is measured by determining ^{47}Sc accumulation in double neutron capture by stable ^{45}Sc nuclei. By measuring the ratio of the activities of ^{47}Sc and ^{46}Sc for a known neutron flux it is possible to determine the cross-section for the ^{46}Sc (n, γ) ^{47}Sc reaction. The ^{47}Sc and ^{46}Sc activities were measured with the help of a semiconductor Ge(Li) gamma spectrometer. The measured cross-section was found to be:

$$\hat{\sigma}\,(^{46}Sc) = 8.3 \pm 1.4 \text{ barn.}$$

The authors also measured the cross-section for ^{64}Cu burn-up. For this purpose, the ^{64}Cu activity growth constant was measured by activation techniques as a function of the irradiation time. The difference between this constant and the ^{64}Cu decay constant is σf, where σ is the cross-section and f the thermal neutron flux. This difference was found to be less than 2%, corresponding to:

$$\hat{\sigma}\,(^{64}Cu) < 6000 \text{ barn.}$$

The authors' estimates show that ^{46}Sc and ^{64}Cu burn-up in thermal neutron fluxes of up to 10^{14} n/cm^2.s does not exceed 1% and may therefore be disregarded.

PHOTODISINTEGRATION OF ^{16}O NUCLEI

V.P. Denisov, A.P. Komar and L.A. Kulchitsky

(article submitted to "Nuclear Physics")

The cross-sections for the ^{16}O (γ, p_{zero}) ^{15}N, ^{16}O (γ, p_{12}) ^{15}N and ^{16}O (γ, p_3) ^{15}N reactions - corresponding to the formation of ^{15}N nuclei in the ground, first + second (5.28 MeV and 5.30 MeV) and third (6.33 MeV) excited states - were determined by analysing photoproton spectra measured for 23 maximum energy values of the gamma emission slowing-down spectrum.

The first column of Table I shows the energies of ^{16}O levels excited in the photo-absorption of gamma quanta. The second and third columns show absolute integral cross-section values and the relative intensities of ^{16}O decay leading to the formation of ^{15}N nuclei in the ground state. The remaining columns show quantities relating to decay to the first + second and third excited states of ^{15}N nuclei.

The integral cross-sections for the corresponding reactions are, within the limits indicated above, as follows:

$$\int_{12.1}^{43} \sigma(\gamma,p_0)\, d\,E\gamma = 47 \pm 6 \text{ MeV mbarn};$$

$$\int_{17.4}^{26.5} \sigma(\gamma,p_{12})\, d\,E\gamma = 10 \text{ MeV mbarn};$$

$$\int_{18.4}^{27.5} \sigma(\gamma,p_3)\, d\,E\gamma = 22 \text{ MeV mbarn}.$$

The integral cross-section for proton formation in all possible reactions is as follows:

$$\int_{12.1}^{55} \sigma_p\, d\,E\gamma = 152 \pm 22 \text{ mbarn MeV}.$$

Table I

RATE OF TRANSITIONS TO VARIOUS STATES OF THE ^{15}N NUCLEUS

MeV	Ground state		First and second excited states (5.28 and 5.30 MeV)		Third excited state (6.33 MeV)	
	MeV. mb	l_o, %	MeV. mb	$l_{1.2}$ %	MeV. mb	l_3, %
17.13 17.29	2.0	100	-	-	-	-
19.0	1.2	55	-	-	1	45
19.5	2.2	35	2.4	40	1.5	25
20.9	3.2	52	-	-	3.0	48
21.7	1.7	56	1.6	12	5.5	32
22.3	8.0		0.6			
23.1	2.7	35	0.5	7	4.4	58
24.3	6.0	53	1.5	13	3.8	34
25.0	2.7	80	-	-	0.7	20
25.6	1.2	20	3.3	52	1.8	28
26.3 27.4	2.5	100	-	-	-	-
28.7 29.6	2.3	37	-	-	4.0	63

EXCITED STATES OF ^{134}Cs

A.M. Berestovoy, I.A. Kondurov and Yu. E. Loginov

The arrangement of the energy levels of ^{134}Cs nuclei obtained in the ^{133}Cs (n, γ) ^{134}Cs reaction has been studied using a gamma-gamma coincidence spectrometer. NaI(Tl) crystals with FEU-13 photomultipliers were used as gamma detectors. During the experiment one of these was replaced by a 1-cm^3 lithium-drifted germanium detector.

It was shown that 116-keV and 176-keV gamma transitions occur from a level with a half-life of 49 $\pm$ 3 ns, while the 240-keV gamma transition occurs from a level with a half-life of 8.0 $\pm$ 1.5 ns.

The most intensive gamma transitions are included in the level scheme constructed by the authors. The binding energy of neutrons in ^{134}Cs nuclei was found to be 6892 $\pm$ 4 keV.

GAMMA EMISSION IN THE ^{76}Se (n, γ) ^{77}Se REACTION

I.A. Kondurov and Yu.E. Loginov

Hard and soft gamma emission in the ^{76}Se (n, γ) ^{77}Se reaction was studied using 8-cm^3 and 4-cm^3 lithium-drifted germanium detectors. Table I shows the energies and absolute intensities of the gamma transitions and their arrangement within the scheme of ^{77}Se excited states.

Table I

Nos.	Transition energy (keV)	Intensity (quanta per 100 captures)	Location of transition in the scheme of excited states of ^{77}Se	
1	88	2.0	249	161
2	125	0.7	300	175
3	139	5.2	300	161
4	161	6.2	161	0
5	199	2.8	438	238
6	238	15.4	238	0
7	249	4.3	249	0
8	282	0.7	521	238
9	296	2.2	818	521
10	438	2.2	438	0
11	521	12.1	521	0
12	569	1.4	818	249
13	580	2.0	818	238
14	649	0.7		
15	755	1.8		
16	819	1.7	818	0
17	889	3.6	1412	521
18	950	1.3	1188	238
19	1011	1.5	1011	0
20	1179	1.4	1618	438
21	1206	2.8		
22	1303	2.9	1823	521
23	1380	0.7	1618	238
24	1414	5.3	1412	0
25	1581	3.0	1823	238
26	5593	1.7	7417	1823
27	5793	1.1	7417	1618
28	6008	2.8	7417	1412
29	6230	0.8	7417	1188
30	6409	1.8	7417	1011
31	6596	5.5	7417	818
32	7178	2.4	7417	238
33	7417	3.4	7417	0

Physics Institute of the Ukrainian SSR Academy of Sciences

NORMALIZED DISTANCES BETWEEN LEVELS OF CERTAIN ISOTOPES AND ISOBARS IN THE REGION OF DEFORMED NUCLEI

V.P. Vertebny, N.L. Gnidak, A.I. Kalchenko, V.V. Koloty, E.A. Pavlenko, M.V. Pasechnik and Zh.I. Pisanko

Data on nuclear level densities obtained by measuring the transmission of samples using mechanical choppers or other pulsed neutron sources provide valuable information about the properties of single-particle levels - e.g. the degree of degeneration of such levels, the distance between them and the extent to which they are filled. The residual interaction - the so-called pair interaction energy - also plays an important part. Unfortunately, all these properties exert a combined influence and the separation of their individual effects depends very largely on the degree of perfection of the nuclear theories employed. It is therefore worth investigating changes in level density at a particular excitation energy as a function of Z and of N for a large number of isotopes. The study of the neutron cross-sections of such rare isotopes as ^{162}Er, ^{164}Er and ^{156}Dy substantially increases the amount of information available on such uncommon Z-N combinations.

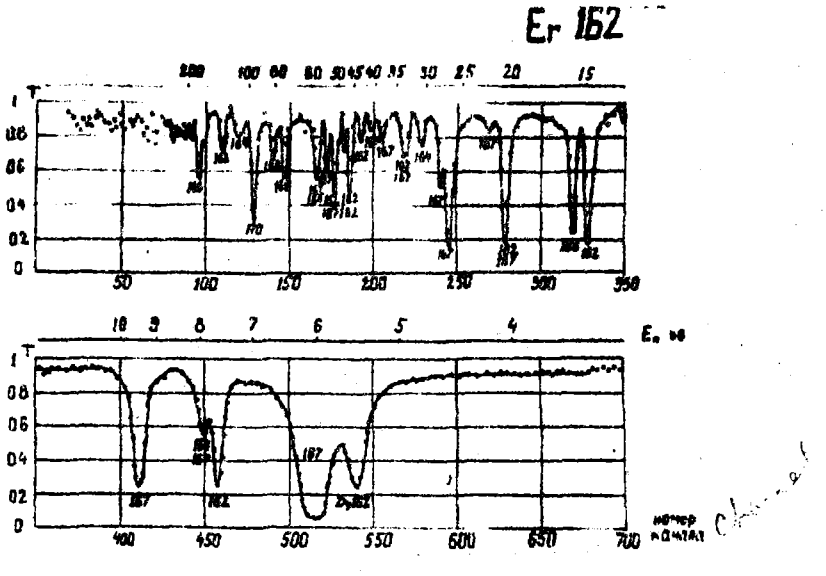

Fig. 1.

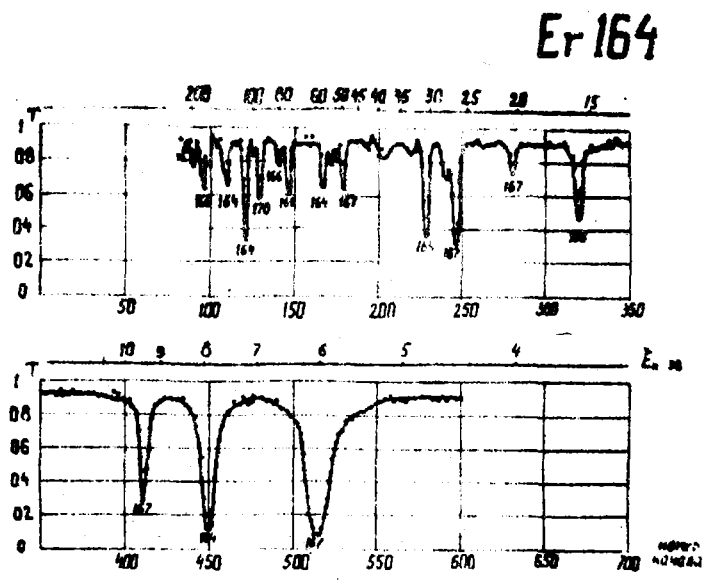

Fig. 2.

Table 1 and Figs 1 and 2 show the observed distances between the levels of certain deformed nuclei and their normalized values for an excitation energy of 6 MeV. The normalized distances between the levels, D_o, are obtained from the experimental values by means of the following formula:

$$D_o = (2I + 1)D_{obs} \left(\frac{\sigma}{U}\right)^2 \exp 2 \left(\sqrt{aU} - \sqrt{\sigma a}\right),$$

where I is the spin of the compound nucleus and U the excitation energy (in MeV).

D_{obs} agrees with the observed distances between levels without multiplication by two in the case where the spin of the target nucleus $I \neq 0$, since the theoretical formulas generally include both parities, whereas levels of one parity are observed in neutron capture. The parameter a is taken from [1]. In the case of erbium isotopes, the distances are obtained from the authors' own measurements (Table 2), performed in a nuclear reactor and with a resolution of 0.05 μs/m. The distances for ^{162}Dy and ^{165}Ho are taken from [1].

It should be noted that the 5.44-eV level attributed to ^{162}Er in [2] belongs to ^{162}Dy (as some of the authors of the present work had previously supposed [3]). The increase in resolution compared with [3] has made it possible to determine the neutron widths of the ^{162}Er and ^{164}Er levels with much greater precision. A radiation width of 88 MeV has been used in calculation. The force functions $\bar{\Gamma}_n^o/\bar{D}$ are $(1.71 \pm^{1.6}_{0.7}) \times 10^{-4}$ for ^{162}Er and $(4.9 \pm^{3.9}_{1.6}) \times 10^{-4}$ for ^{167}Er.

Although the exact value of the derived distances depends on the method of normalization (see, for example, [1] and [4]), the general tendency of D to change with increasing N remains the same in all cases. This tendency is apparently connected with the existence of a sub-shell at N = 100.

Table 1

Derived distances between levels

Nucleus	Compound nucleus Z	Compound nucleus N	a	$E_{binding}$	U	$D_{exp.}$	D_o
^{162}Er	68	95	22.31	6.844	6.220	7.3 ± 1.8	10.2 ± 2.5
^{164}Er	68	97	21.404	6.644	6.024	30 ± 8	32 ± 8
^{166}Er	68	99	20.668	6.438	5.818	53 ± 14	40 ± 11
^{167}Er	68	100	20.19	7.769	6.54	4.0 ± 0.5	58 ± 7

where $E_{binding}$ is the energy of neutron separation from the compound nucleus and U the effective excitation energy = E-P(N)-P(Z), P being the pair interaction energy of a nucleon (all in MeV).

Table 2

Resonance parameters of erbium isotopes

Erbium-162

E_o (eV)	Γ_n^o (MeV)	E_o (eV)	Γ_n^o (MeV)
7.60 ± 0.03	0.23 ± 0.03		
14.74 ± 0.06	0.81 ± 0.07	46.2 ± 0.5	1.35 ± 0.26
20.5 ± 0.14	0.71 ± 0.08	47.7 ± 0.5	0.40 ± 0.09
33.6 ± 0.3	0.23 ± 0.03	51.0 ± 0.5	3.0 ± 0.6
42.9 ± 0.4	0.17 ± 0.05	57.9 ± 0.6	3.7 ± 1.2
		132 ± 3	4.4 ± 1.4

Erbium-164

E_o (eV)	Γ_n^o (MeV)	E_o (eV)	Γ_n^o (MeV)
7.88 ± 0.003	0.23 ± 0.04	57.2 ± 0.6	
30.7 ± 0.3	0.6 ± 0.2	109 ± 1.5	
		129 ± 3	

Erbium-166

E_o (eV)	Γ_n^o (MeV)	E_o (eV)	Γ_n^o (MeV)
15.67 ± 0.07	0.55 ± 0.06	85 ± 1	
74.9 ± 1		173 ± 3	

Erbium-167

E_o (eV)	$2g\Gamma_n^o$ (MeV)	E_o (eV)	$2g\Gamma_n^o$ (MeV)
0.46		33.0 ± 0.2	0.7 ± 0.3
0.58		37.6 ± 0.2	0.8 ± 0.15
5.97 ± 0.01	10.6 ± 1.3	39.7 ± 0.2	0.7 ± 0.15
7.94 ± 0.02	0.14 ± 0.05	42.2 ± 0.2	
9.45 ± 0.02	2.2 ± 0.2	49.8 ± 0.2	1.3 ± 0.1
20.3 ± 0.06	1.3 ± 0.2	53.3 ± 0.3	4.8 ± 0.4
22.06 ± 0.07		59.7 ± 0.4	1.3 ± 0.25
26.2 ± 0.1	28 ± 5	62.2 ± 0.4	1.9 ± 0.4
27.5 ± 0.1	1.1 ± 0.4		

REFERENCES

1. GILBERT, A., CAMERON, A.G.W., Can. Jour. Phys. 43, 1446 (1965).

2. CLAIEN et al. Bull. Am. Phys. Soc., II, 300 (1966).

3. VERTEBNY B.P. et al. The International Conference on the Study of Nuclear Structure with Neutrons. Antwerp, Belgium, July, 19-23 (1965).

4. GORDEEV, I.V., KARDASHEV, D.V., MALYSHEV, A.V., Jaderno-fizičeskie konstanty (Nuclear physics constants), (1963).

ENERGY DEPENDENCE OF THE CROSS-SECTION FOR THE SCATTERING OF COLD NEUTRONS BY LIQUID GALLIUM IN THE WAVELENGTH RANGE 1-8 A

V.P. Vertebny, V.A. Gulko, A.N. Maistrenko and V.F. Razbudey

(article submitted to "Ukr. fiz. Ž.")

Using the time-of-flight method, the authors have measured the total neutron cross-section for liquid gallium (sample temperature $31^{\circ} \pm 0.5^{\circ}$C) in the Physics Institute's WWR-M reactor. The resolution was ~ 20 μs/m. The thickness of the sample was 4.159×10^{22} nuclei/cm^2. The scattering cross-section was obtained from total cross-sections by subtracting the absorption cross-section on the assumption that it changes in accordance with the 1/υ law. A value of $\sigma_a = 2.77$ barn was taken for $\upsilon = 2200$ m/s [1]. Data on scattering cross-sections as a function of λ are presented in Table 1.

Using X-ray diffraction data for liquid gallium [2], the authors calculated the coherent scattering cross-section by means of the formula

$$\sigma_{coh}(\lambda) = 8\pi a^2 \coh\left(\frac{\lambda}{4\pi}\right)^2 \int_0^{\frac{4\pi}{\lambda}} S \cdot i(s)\, dS,$$

where θ is the scattering angle, $S = \frac{4\pi}{\lambda} \sin\frac{\theta}{2}$, and i(S) is the intensity of the X-ray pattern corrected by the atomic form factor and normalized to unity as $S \to \infty$. Experimental values of i(S) were taken from [2]. Fig. 1 shows experimental scattering cross-section values and the theoretical curve.

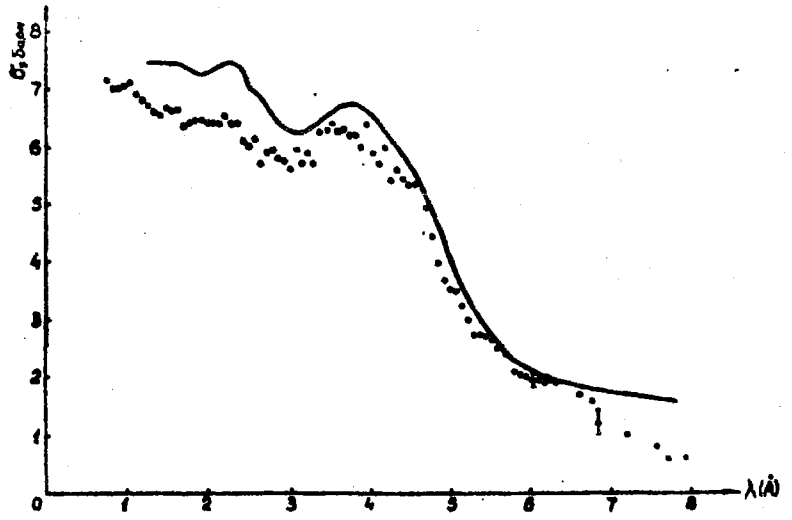

Fig. 1

Table 1

λ (Å)	σ_s (barn)	λ (Å)	σ_s (barn)
1	2	3	4
0.74	7.12 ± 0.07	2.51	5.91
0.81	6.95	2.58	6.05 ± 0.13
0.88	6.93	2.65	5.63
0.96	6.99	2.73	5.80
1.03	7.01	2.80	5.86
1.11	6.90 ± 0.06	2.88	5.68
1.18	6.78	2.95	5.64 ± 0.13
1.25	6.70	3.02	5.53
1.33	6.55	3.10	5.89
1.40	6.49	3.17	5.65
1.47	6.61 ± 0.07	3.24	5.81
1.55	6.57	3.32	6.22 ± 0.19
1.62	6.59	3.39	6.21
1.70	6.30	3.47	6.82
1.77	6.36	3.54	6.27
1.84	6.38 ± 0.08	3.61	6.14
1.92	6.40	3.69	6.21 ± 0.25
1.99	6.32	3.76	6.05
2.06	6.35	3.83	6.05
2.14	6.37	3.91	5.84
2.21	6.47 ± 0.1	3.98	6.28
2.29	6.36	4.06	5.74 ± 0.34
2.36	6.34	4.13	5.55
2.43	6.05	4.20	5.86
4.28	5.28	5.83	2.01
4.35	5.48	5.90	1.97 ± 0.25
4.42	5.36 ± 0.41	5.97	1.96
4.50	5.26	6.05	1.93
4.57	5.36	6.12	1.88
4.65	4.82	6.19	1.79
4.72	5.01	6.27	1.87 ± 0.35

1	2	3	4
4.79	4.41 ± 0.16	6.34	2.02
4.87	3.94	6.42	2.14
4.94	3.66	6.49	2.24
5.01	3.51	6.56	1.82
5.09	3.43	6.64	1.62 ± 0.41
5.16	3.24 ± 0.19	6.71	1.43
5.24	2.92	6.78	1.37
5.31	2.71	6.86	1.10
5.38	2.68	6.93	1.34
5.46	2.65	7.23	1.26 ± 0.6
5.60	2.44 ± 0.23	7.45	1.19 ± 0.6
5.68	2.40	7.60	0.68 ± 0.6
5.75	2.24	7.74	0.42 ± 0.6
		7.97	0.43 ± 0.6

REFERENCES

1. Handbook on nuclear physics (translated from English), Fizmatgiz, Moscow (1963).

2. H. Menke, Phys. Leit., 33, 593 (1932)

   H. Hendus, L.f. Naturforschung., B, 2a, 447 (1947).

PARAMETERS OF THE OPTICAL NUCLEAR MODEL FROM DATA ON ELASTIC SCATTERING OF 1.5-MeV NEUTRONS

I.A. Korzh, I.E. Kashuba, B.D. Kozin and M.V. Pasechnik

(article submitted to "Jadernaja fizika")

The authors present the results of an analysis (based on a local six-parameter optical model of the nucleus) of experimental data on total and differential cross-sections for the elastic scattering of neutrons with an initial energy of 1.5 MeV by the following nuclei:

Na, Al, P, Ti, Cr, Fe, Co, Ni, Cu, Zn, Zr, Nb, Mo, Ag, In, Sn, Sb, I, Sm, Yb, Ta, W, ^{184}W, Pt, Au, Hg, Tl, Pb, Bi, Th, ^{235}U, ^{238}U.

The optimum values of the parameters V, W and a are determined for fixed values of r_o = 1.25 fm, B = 0.98 fm and V_{SO} = 10 MeV. It is shown that, for deformed nuclei, fitting of the potential parameters of the spherical model does not give agreement between calculated and experimental values.

The table shows the optimum values of the potential parameters, together with calculated and experimental total cross-sections.

Optimum values of the parameters of the optical nuclear model obtained by three-parameter fitting

Element	V MeV	W MeV	a fm	σ_t (calc) barn	σ_t (exp) barn	χ^2
1	2	3	4	5	6	7
Na	47.8	8.3	0.43	2.452	2.45	0.044
Al	47.4	6.3	0.46	3.204	3.20	0.133
P	55.3	7.9	0.54	2.969	3.00	0.416
Ti	49	7.4	0.55	3.212	3.20	5.635
Cr	50.9	8.3	0.37	3.233	3.10	5.269
Fe	49.7	4.9	0.42	2.306	2.80	0.760
Co	49	12.5	0.62	3.305	3.30	0.237

Element	V MeV	W MeV	a fm	σ_t (calc) barn	σ_t (exp) barn	χ^2
1	2	3	4	5	6	7
Ni	47.1	3.5	0.40	3.149	3.10	[illegible]
Cu	50.1	8.1	0.56	3.115	3.10	4.327
Zn	[illegible]	12.6	0.53	3.231	3.25	0.543
Zr	46.7	5.2	0.74	5.559	5.55	[illegible]
Nb	46.9	9.6	0.76	5.662	5.80	2.226
Mo	47.3	9.9	0.74	5.779	5.75	0.199
Ag	47.5	14.8	0.76	5.854	5.85	0.171
In	48.3	7.5	0.67	6.032	6.00	0.923
Sn	48.2	5.0	0.58	6.023	6.00	0.162
Sb	47.4	7.2	0.71	6.479	6.40	0.149
I	44.8	8.3	0.73	6.672	6.70	0.228
Sm	43.2	13.4	0.72	6.802	6.85	1.626
Yb	42.9	16.7	0.72	6.947	6.95	4.616
Ta	41.6	15.3	0.79	7.171	7.25	5.192
W	42.5	21.5	0.87	7.177	7.00	7.194
^{184}W	45.3	20.3	0.65	6.276	6.30	5.824
Pt	47.6	12.1	0.58	5.831	5.65	4.681
Au	46.6	8.7	0.69	5.921	5.85	3.394
Hg	45.8	8.9	0.73	6.125	6.00	1.612
Tl	47.2	7.8	0.67	5.771	5.25	31.173
Pb	46.9	5.3	0.52	5.371	5.30	0.915
Bi	47.3	3.9	0.38	5.185	5.10	2.380
Th	41.7	10.3	0.60	6.258	6.60	10.858
^{235}U	45	10.7	0.61	6.417	6.70	9.434
^{238}U	43.4	12	0.58	6.440	7.00	5.533

RESONANCES OF THE RARE ISOTOPES ^{156}Dy, ^{158}Dy AND ^{160}Dy

V.P. Vertebny, N.L. Gnidak, A.I. Kalchenko, V.V. Koloty,
E.A. Pavlenko, M.V. Pasechnik, Zh.I. Pisanko
and V.K. Rudyshin

With a resolution of 0.055 and 0.22 μs/m, the authors measure, in the Physics Institute's WWR-M reactor, the transmission of dysprosium oxide samples enriched to ~ 18% in ^{156}Dy, ~ 14% in ^{158}Dy and ~ 68% in ^{160}Dy for neutron energies of 0.5-1000 eV.

To facilitate identification of levels, the authors also measure the transmission of natural dysprosium. The results are summarized in Table 1. The identification of levels, and in particular the determination of neutron widths, is particularly difficult owing to the high level density of ^{161}Dy and ^{163}Dy. Above 20 eV, the values of Γ_n are therefore only tentative. The levels for ^{158}Dy are detected only after area analysis of the resonances.

Estimates show that, in the energy range 14-50 eV, levels with a neutron width less than 3 MeV in the case of ^{156}Dy and less than 7 MeV in the case of ^{158}Dy may have been omitted due to the fact that the resonances of different isotopes coincide. Levels which coincide with the levels of abundant isotopes are marked by an asterisk. The strength function $\frac{\overline{\Gamma_n}^o}{\overline{D}}$ $^{156}Dy \approx 2.2 \times 10^{-4}$.

The observed distances between levels and those normalized to an excitation energy of 6 MeV (I = 0) by means of the formula

$$D_{norm} = (2I + 1)D_{obs}\left(\frac{g}{u}\right)^2 \exp 2\left(\sqrt{aU} - \sqrt{6a}\right)$$

are presented in Table 2 (I - spin of compound nucleus, U - excitation energy (MeV), a - parameter taken from [1]). The normalization formula applies to the case where $I \neq 0$. When I = 0, it is necessary to add the coefficient $\frac{1}{2}$ to the right-hand side of the formula.

Table 1

Isotope		E_o eV	Γ_n MeV	Γ_n^o MeV	Γ_γ MeV	Comments
Dysprosium-156	1	2.15 ± 0.02	0.2 ±	0.148 ±		
	2	3.21 ± 0.01	0.8 ± 0.2	0.45 ± 0.11	158 ±	Γ_γ determined by the line width
	3	9.19 ± 0.04	0.6 ± 0.15	0.19 ± 0.05	108 ± 10	"
	4	15.2 ± 0.1	4.6 ± 0.7	1.2 ± 0.2	-	
	5	17.4 ± 0.1	0.32 ± 0.2	0.08 ± 0.05	-	
	6	17.7 ± 0.1	0.1 ± 0.1	0.02 ± 0.02	-	
	7	19.6 ± 0.1	9 ± 2	2.1 ± 0.5	-	
	8	24.5 ± 0.2	~2.4	~0.48	-	For this and all subsequent levels, the neutron width is determined in the zero approximation and given as an indication of the resonance characteristics
	9	27.4 ± 0.2	0.4 ± 0.4	0.08 ± 0.08	-	
	10	28.1 ± 0.2	0.4 ± 0.4	0.08 ± 0.08	-	
	11	29.3 ± 0.25	~8.7	~1.6	-	
	12	36.0 ± 0.3	~9	~1.5	-	
	13	37.8 ± 0.4	-	-	-	Γ = 34 MeV if there is only one level in the range 37.8-38.6 eV
	14	38.6 ± 0.4	-	-	-	
	15	46.9 ± 0.5	~14	~2	-	
	16	52.0 ± 0.6	~16	~2	-	
	17	68.6 ± 0.6	~54	~6.5	-	
	18	85.5 ± 1.2	~15	~1.7	-	
	19	90.7 ± 1.4	~42	~4	-	"Strong" level or group of "strong" levels
	20	124 ± 2	-	-	-	

Table 1

(continued)

Isotope		E_o MeV	Γ MeV	Γ^o MeV	Γ MeV	Comments
Dysprosium-158	1	38 ± 1 (a)	~22	~3.6	-	(a) Identification not final
	2	45.6 ± 0.5	~39	~5.7	-	
	3	59.7 ± 0.7 (a)	-	-	-	
	4	86 ± 1.5 (b)	~81	~8.7	-	(b) Identification not final; the levels may belong to dysprosium-161
	5	172 ± 3 (b)	-	-	-	
	6	271 ± 4 (b)	-	-	-	
Dysprosium-161	1	1.88 ± 0.02	0.4 ± 0.2	-	-	
	2	7.72 ± 0.03	-	-	-	The level has 60-MeV less energy than the corresponding level of dysprosium-161
	3	10.4 ± 0.05*	19 ± 3	5.9 ± 0.9	-	
	4	20.5 ± 0.1*	~25	~5.6	-	
	5	35 ± 0.3*	-	-	-	
	6	85 ± 1.5	~93	~10	-	

Table 2

Isotope dysprosium	$D_{obs.}$ (eV)	$D_{norm.}$ (eV)	$D_{calc.}$ (eV) not normalized
156	3.4 ± 0.4	2.8	9.4
158	$30 \pm {}^{12}_{5}$ (a)	$27 \pm {}^{11}_{4}$	15.4
160	$11 \pm {}^{9}_{5}$	$5 \pm {}^{4}_{2.3}$	50
161	2.2	22	2.3
162	42 ± 6 (1)	15	100
163	9 ± 1	36	11
164	-	-	370

(a) The errors in the level spacings of dysprosium-156, dysprosium-158 and dysprosium-160 are obtained from histograms of the number of levels against the level energy. No correction was made for omitted levels.

REFERENCES

[1] A Gilbert, A.G.W. Cameron, Canadian Journal of Physics 43 (1965) 1446.

V.G. Khlopin Radium Institute

CROSS-SECTIONS AND RESONANCE INTEGRALS FOR THE CAPTURE AND FISSION OF LONG-LIVED AMERICIUM ISOTOPES

M.A. Bak, A.S. Krivokhatsky, K.A. Petrzhak,
Yu.G. Petrov and E.A. Shlyamin

(article submitted to "Atomnaja energija")

Targets of ^{241}Am (99.9% ^{241}Am+0.1% ^{239}Pu) and ^{241}Am + ^{243}Am (7.5% ^{241}Am + 91.5% ^{243}Am) are irradiated in the vertical channels of the WWR-M reactor in neutron fluxes of (1.5-10) x 10^{13} $n/cm^2.s$ for a period of 5-100 h for the purpose of observing an approximately tenfold increase in alpha activity due to accumulated products (^{242}Cm and ^{244}Cm).

From the increase in alpha activity of the irradiated targets and the change in the fission count rate in a double ionization chamber the authors find the capture and fission cross-sections for ^{241}Am, ^{242}Cm and ^{243}Am.

Through simultaneous bombardment of targets with and without cadmium plating it is possible to determine the corresponding resonance integrals. The results are summarized in Table 1.

Table 1

Isotope	Cross-section (barn)	Resonance integral (barn)
^{241}Am	$\sigma_c' = 670 \pm 60$	$RI_c^1 = 2100 \pm 200$
	$\sigma_c'' = 70 \pm 5$	$RI_c'' = 300 \pm 30$
	$\sigma_f = 3.15 \pm 0.10$	$RI_f = 21 \pm 2$
^{242}Am	$\sigma_f = 2100 \pm 200$	$RI_f < 300$
^{243}Am	$\sigma_c = 73 \pm 6$	$RI_c = 2300 \pm 200$

NEUTRON FISSION CROSS-SECTION OF ^{226}Ra AND ANGULAR DISTRIBUTIONS OF THE FRAGMENTS

Yu.A. Babenko, Yu.A. Nemilov,
Yu.A. Solitsky and V.B. Funshtein

The authors measure the cross-sections for ^{226}Ra fission by neutrons with energies of 3-15 MeV and the angular distributions of fragments resulting from radium fission by neutrons having an energy of 6.7, 8.9, 11.6, 12.5, 13.6, 14.4 and 14.8 MeV. Up to 6 MeV, the effective energy of the neutrons was determined to within $\pm$ 0.1 MeV, and at higher energies to within $\pm$ 0.2 MeV. The fission cross-section does not vary monotonically. It follows from the curve that the ^{227}Ra and ^{226}Ra fission barriers are 8.5 $\pm$ 0.5 MeV. The measured anisotropy of the divergence of the fission fragments confirms the presence of emissive fission at $E_n > 9$ MeV. The shape of the angular distribution of fragments resulting from radium fission by neutrons having an energy of 14.4-14.8 MeV indicates that there is an increased fission fragment yield at ~ 60° to the neutron beam.

Table 1

Cross-section for ^{226}Ra fission by neutrons

E_n (MeV)	σ_f (mbarns)
3.0	(40 $\pm$ 20). 10^{-3}
3.3	0.4 $\pm$ 0.1
3.5	0.6 $\pm$ 0.1
3.8	1.5 $\pm$ 0.2
4.3	1.7 $\pm$ 0.3
5.4	2.7 $\pm$ 0.4
6.0	3.0 $\pm$ 0.5
6.7	3.1 $\pm$ 0.5
8.0	3.3 $\pm$ 0.5
8.9	3.5 $\pm$ 0.5
9.6	3.9 $\pm$ 0.8
10.3	5.4 $\pm$ 0.8
11.5	6.6 $\pm$ 1.0
12.5	9 $\pm$ 1
13.6	12 $\pm$ 2
14.0	14 $\pm$ 2
14.4	15 $\pm$ 2
14.8	17 $\pm$ 2

Table 2

Angular distribution of fragments resulting from ^{226}Ra fission by neutrons

Values of $\frac{\sigma_f(\theta^\circ)}{\sigma_f(90^\circ)}$

	E_n = 6.7 MeV	E_n = 8.9 MeV	E_n = 11.6 MeV	E_n = 12.5 MeV
11°	1.97	1.07	1.1	1.3
21°	1.72	1.2	1.13	1.59
34°	1.64	1.06	1.22	1.36
47°	1.5	1.43	1.14	1.43
61°	1.34	1.07	1.04	1.09
76°	1.05	0.88	0.96	0.94
90°	1.03	1.07	1.08	1.03

	E_n = 13.6 MeV	E_n = 14.4 MeV	E_n = 14.8 MeV
11°	1.38	1.61	1.64
16°	1.38	1.27	1.58
23°	1.47	1.32	1.36
31°	1.37	1.11	1.29
39°	1.42	1.04	1.44
47°	1.15	1.17	1.33
55°	1.32	1.41	1.47
64°	1.05	1.37	1.47
73°	1.17	0.9	1.34
81°	0.99	0.94	1.08
90°	1.05	1.16	1.0

For E_n = 6.7, 8.9, 11.6, 12.5, 13.6 and 14.4 MeV $\frac{\sigma_f(\theta^\circ)}{\sigma_f(90^\circ)}$ is determined to within $\pm$ 15%; for E_n = 14.8 MeV it is determined to within $\pm$ 10%.

YIELD AND ANGULAR ANISOTROPY OF ^{226}Ra PHOTOFISSION FRAGMENTS

E.A. Zhagrov, Yu.A. Nemilov and Yu.A. Selitsky

Using the mica chip method for recording fission fragments, the authors measure the relative yield of ^{226}Ra photofission in the effective gamma energy E_0 range of 9-25 MeV [1]. On the basis of ^{238}U data, they establish the dependence of the ^{226}Ra photofission yield per roentgen per target nucleus as a function of the effective gamma energy E_0.

The ^{226}Ra photofission threshold is found to be 8.5 ± 0.5 MeV. The angular dependences of the fission fragments, measured by the mica chip method, show that for given excitation energies above the threshold the anisotropy is less in the case of radium than in that of ^{232}Th. The authors give the dependence of the anisotropy coefficient a as a function of the bremsstrahlung effective gamma energy (Table 2).

Table 1

Energy E_0, MeV	Relative yield $^{226}Ra/^{238}U$
25	$6.3 \cdot 10^{-3} \pm 3 \cdot 10^{-4}$
19	$5.9 \cdot 10^{-3} \pm 3 \cdot 10^{-4}$
16	$5.2 \cdot 10^{-3} \pm 4 \cdot 10^{-4}$
10.7	$2.3 \cdot 10^{-3} \pm 2 \cdot 10^{-4}$
9.1	$4.8 \cdot 10^{-4} \pm 7 \cdot 10^{-5}$
8.3	$2.8 \cdot 10^{-4} \pm 5 \cdot 10^{-5}$

Table 2

Energy E_0, MeV	Anisotropy coefficient a
26	0.07 ± 0.03
22	0.16 ± 0.04
18	0.34 ± 0.08
14.5	0.65 ± 0.22
10.7	2.3 ± 0.7
9.1	6.1 ± 2.7

V.G. Khlopin Radium Institute
Joint Institute for Nuclear Research

GAMMA EMISSION BY ^{81}Rb, $^{82*}Rb$, ^{82}Rb, ^{83}Rb, ^{84}Rb and ^{86}Rb

J. Vrzal, B.S. Dzhelepov, A.G. Dmitriev, N.N. Zhukovsky,
J. Liptak, L.N. Moskvin, J. Urbanec, L.G. Tsaritsyna

(article submitted to "Izv. Akad. Nauk SSSR, Ser. fiz.")

Using germanium-lithium detectors with sensitive volumes of ~ 5 cm^3 and ~ 13.5 cm^3, the authors investigate the gamma emission of rubidium isotopes with A = 81, 82 (isomer), 82, 83, 84 and 86. The rubidium fraction is separated from strontium and yttrium targets bombarded with fast protons (E_p ~ 660 MeV) through preliminary separation of the accompanying elements by co-precipitation and distributive chromatography.

Dowex-50 is used for final purification of the preparation. The energies and relative intensities of the gamma lines are determined (Table 1). Five new lines ($h\nu$ = 712, 1384, 2162, 2413 and 2480 keV) are found in the gamma spectrum of ^{82}Rb. The decay schemes of $^{82*}Rb$ and ^{82}Rb are determined with greater precision. Three excitation levels, with energies of 2162, 2480 and 3190 keV, are added to the decay scheme of ^{82}Rb. The percentages of β^+ decay and orbital electron capture events are determined (Figs 1 and 2).

The authors also determine the experimental yields of reactions resulting from deep penetration into yttrium by protons with E_p ~ 660 MeV which lead to the formation of rubidium radioisotopes (Table 2). Deviations of the experimental cross-sections for deep penetration reactions from cross-sections calculated on the basis of Rudstam's semi-empirical formulas do not exceed 30%.

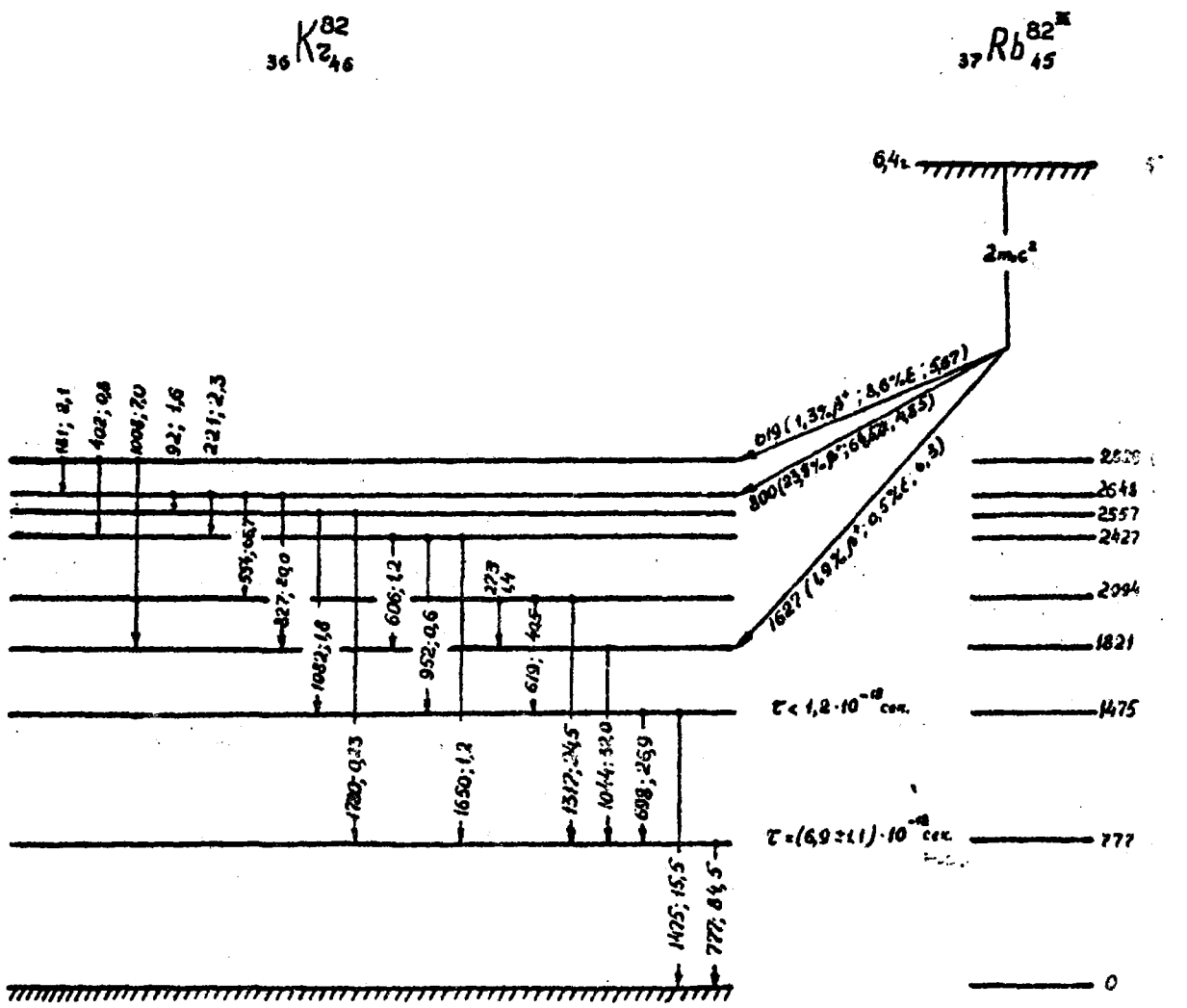
$_{36}Kr^{82}_{46}$
$_{37}Rb^{82m}_{45}$
6,4
$2mc^2$
181; 8,1
402; 9,8
1008; 20
92; 1,6
221; 2,3
819 (1,3% β^+; 8,6% ε; 587)
800 (23,8% β^-; 6,6% ε; 435)
1627 (4,9% β^-; 0,5% ε; 0,5)
554; 0,7
827; 2,0
1082; 1,8
606; 1,2
952; 0,6
223
1,4
445
619;
1780; 0,3
1650; 1,2
1312; 2,5
1044; 3,0
698; 2,9
1425; 15,5
777; 84,5
$\tau < 1{,}2 \cdot 10^{-10}$ sec.
$\tau = (6{,}9 \pm 1{,}1) \cdot 10^{-10}$ sec.
2648
2557
2427
2094
1821
1475
777
0

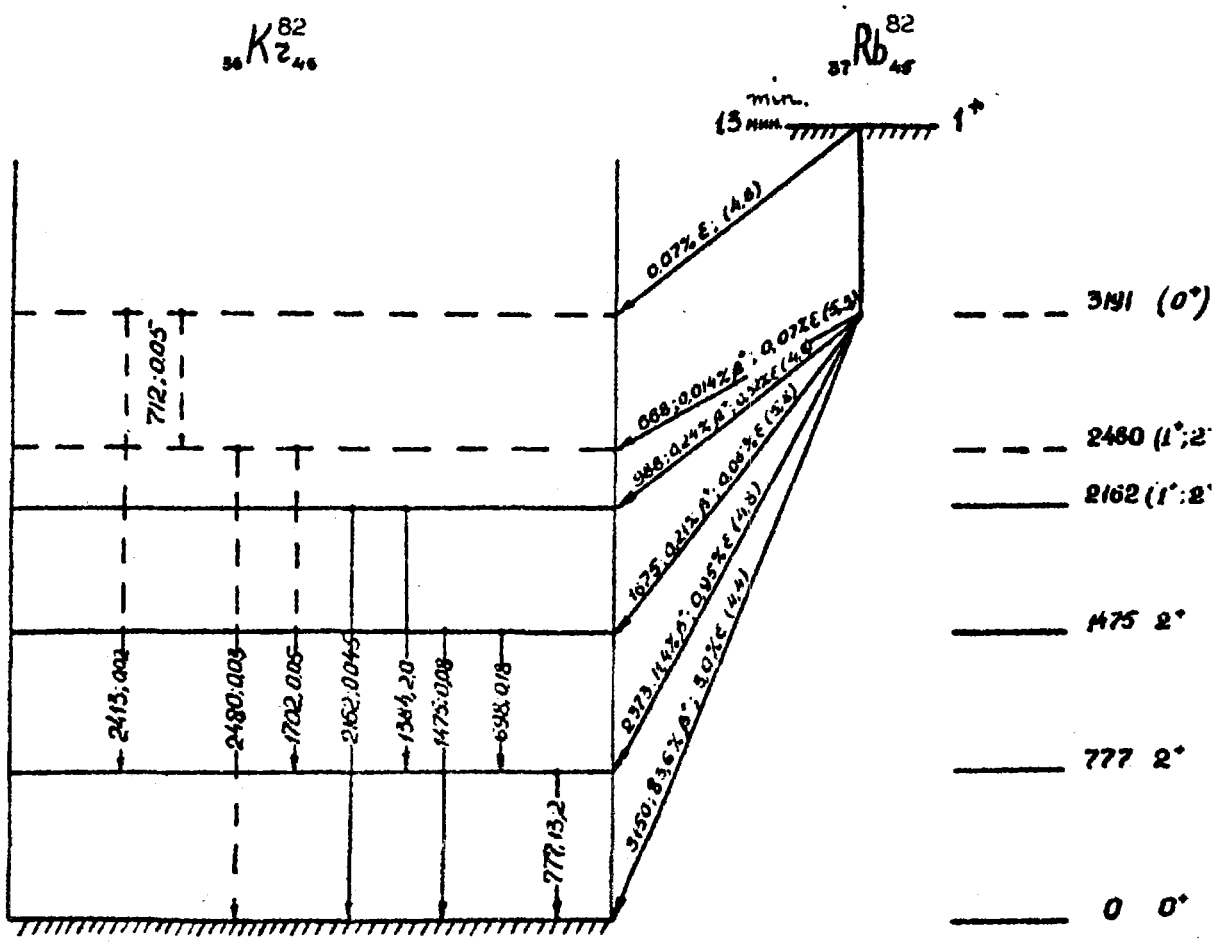
$_{36}Kr^{82}_{46}$
$_{37}Rb^{82}_{45}$
13 min.
1+
0.07% ε ; (4.8)
712; 005
668; 0.014% β⁺ ; 0.07% ε (5.3)
986; 0.44% β⁺ ; 0.12% ε (4.9)
1625; 0.21% β⁺ ; 0.06% ε (5.8)
2323; 1.46% β⁺ ; 0.15% ε (4.8)
3150; 83.6% β⁺ ; 3.0% ε (4.4)
2413; 002
2480; 003
1702; 005
2162; 0.045
1364; 20
475; 0.08
638; 018
777; 13.2
3NI (0⁺)
2480 (1⁺;2
2162 (1⁺;2
475 2⁺
777 2⁺
0 0⁺

Table 1

Energies and relative intensities of the gamma lines of rubidium isotopes

$^{81}Rb(T_{\frac{1}{2}} = 4.7\ h)$		$^{82*}Rb(T_{\frac{1}{2}} = 6.4\ h)$		$^{82}Rb(T_{\frac{1}{2}} = 1.3\ min)$		$^{83}Rb(T_{\frac{1}{2}} = 83\ days)$		$^{84}Rb(T_{\frac{1}{2}} = 33\ days)$	
hν keV	I_γ	hν keV	I_γ	hν keV	I_γ	hν keV	I_γ	hν keV	I_γ
190	100	92	0.9 ± 0.2	511	1452 ±90	520	100	883	100
446	24.3	181	1.6 ± 0.5	698	1.35 ± 0.08	530	65.7 ± 1.5	1020	0.61 ± 0.07
		221	2.7 ± 0.5	712	0.36 ± 0.04	553	37.6 ± 1.5	1900	1.10 ± 0.07
		273	1.6 ± 0.3	777	100	792	1.49 ± 0.08		
		402	0.9 ± 0.2	1384	3.98 ± 0.15	802	0.72 ± 0.08		
		454	1.6 ± 0.4	1475	0.63 ± 0.03				
		554	79 ± 2	1702	0.42 ± 0.03				
		606	2.0 ± 0.2	2162	0.34 ± 0.03				
		619	48 ± 2	2412	0.15 ± 0.02				
		698	32 ± 1	2480	0.22 ± 0.05				
		777	100						
		828	24 ± 1						
		952	0.68 ± 0.07						
		1008	8.3 ± 0.1						
		1082	2.1 ± 0.1						
		1044	37.9 ± 1.5						
		1317	29 ± 1						
		1475	18.3 ± 0.9						
		1650	1.39 ± 0.15						
		1780	0.27 ± 0.04						
		1823	0.03 ± 0.01						
		1876	0.04 ± 0.01						
		1960	0.06 ± 0.01						
		2057	~0.02						

Table 2

Relative yields of rubidium isotopes from yttrium target

Isotope	Relative yield	Cross-section (in mbarn)	
		Authors' results	Rudstam's results
^{81}Rb	100.7 ± 3.1	38.9	39.3*/
$^{82*}Rb$	100	38.7	38.7
^{83}Rb	83.5 ± 0.8	32.3	31.9
^{84}Rb	53.2 ± 0.7	20.6	18.6
^{86}Rb	7.71 ± 0.08	2.98	2.28

*/ Cumulative yield of entire chain:

$^{81}Zr \rightarrow {}^{81}Y \rightarrow {}^{81}Sr \rightarrow {}^{81}Rb$

Joint Institute for Nuclear Research

DETERMINATION OF THE SPINS OF ^{165}Ho NEUTRON RESONANCES

V.P. Alfimenkov, V.I. Lushchikov, V.G. Nikolenko,
Yu.V. Taran and F.L. Shapiro

(JINR preprint P3-3208, Dubna, 1967)

The authors measure the transmission of polarized neutrons through a polarized holmium target using a time-of-flight neutron spectrometer with a resolution of 25 ns/m. From these measurements they determine the spin, I, of 18 excited states of the compound nucleus ^{165}Ho corresponding to neutron resonances at the following energies: 21.0 (I = 4); 35.3 (3); 37.0 (4); 39.4 (4); 47.3 (3); 51.2 (3); 64.7 (4); 71.4 (4); 93.6 (4); 101.9 (4); 106.3 (4); 117.7 (4); 83.9 (4); 84.8 (3); 85.7 (3); 126.8 (3); 128.4 (3) and 150.9 (3).

RADIATIVE CAPTURE OF NEUTRONS BY NUCLEI WITH A = 140-200

V.A. Konks, Yu.P. Popov and Yu.I. Fenin

(JINR preprint P3-3417, Dubna, 1967)

From spectrometer measurements of the slowing-down time of neutrons in lead the authors find the dependence of the cross-sections for the radiative capture of neutrons with energies up to 50 keV by europium, europium-153, holmium-165 and lutetium nuclei. By analysing the energy dependence of the averaged capture cross-sections they obtain strength function values for s- and p-neutrons (see table).

Table I

Results of analysis of averaged capture cross-sections*

Isotope		Other authors						
		So	Sγ	Sl	So	Sγ	Sl	$\bar{S}_l$
Eu_{63}	5/2	2.3 + 0.3 (16) 3.3 ± 0.5			3.3 3.2 ± 0.2	107 ± 3 113 ± 15	0.6 ± 0.3 0.45 ± 0.31	0.5 ± 0.4
^{151}Eu	5/2	3.4 ± 0.9 (16) 2.7 ± 0.5	100 (7)		4.0 4.1 ± 0.3	107 ± 3 115 ± 20	0.9 ± 0.5 1.0 ± 0.8	1 ± 0.8
^{153}Eu	5/2	1.8 ± 0.6 2.7 ± 0.6 (16)	62 (7)		2.5 2.5 ± 0.2	108 ± 4 105 ± 20	0.6 ± 0.3 0.6 ± 0.4	0.6 ± 0.4
$^{165}Ho_{67}$	7/2	2.5 ± 0.4 (16.7)	6.9(7)	0.4 ± 0.4(1)	2.5 1.9 ± 0.4 2.5	11.2 ± 0.4 14.1 ± 3.2 11.1 ± 0.5 10 ± 4	1.7 ± 0.3 1.1 ± 0.5 1.8 ± 0.5	1.5 ± 0.9
Lu_{71}	7/2	1.7 ± 0.2 (16.7)	107 (7)	0.1 ± 0.1(1)	1.7 1.35 ± 0.05	15.3 ± 0.3 23.4 ± 1.7	0.76 ± 0.10 0.18 ± 0.08	0.5 ± 0.4

*All parameters in units of 10^{-4}

MEASUREMENT OF THE RATIO OF FISSION AND RADIATIVE CAPTURE CROSS-SECTIONS FOR ^{235}U AND ^{239}Pu IN THE RESONANCE REGION OF NEUTRON ENERGIES

Yu.V. Ryabov, So Don Sik, N. Chikov and N. Yaneva

Using the Institute's pulsed fast reactor and the time-of-flight method, with a resolution of 0.4, 0.25, 0.06 and 0.04 μs/m, the authors measure fission cross-sections $\sigma_f(E)$ and $\alpha = \frac{\sigma_c(E)}{\sigma_f(E)}$ for ^{239}Pu in the neutron energy region 5 eV-23 keV and for ^{235}U in the energy region 0.15 eV-30 keV.

A liquid scintillation detector with cadmium introduced into the solution is used for performing the measurements. The fission events are registered by recording the delayed coincidences of pulses from prompt gamma rays and the slowed-down fission neutrons. Anticoincidences determine the counting of radiative capture events.

Additional measurements of the cross-section for ^{235}U fission are made using a gas scintillation counter and a cylindrical ionization chamber. Figs 1-9 show $\sigma_f(E)$ and $\alpha(E)$ for ^{235}U and ^{239}Pu. Fission and radiative cpature resonance integral values for the energy ranges of interest when one is compiling multi-group constants for reactor calculations are presented in Tables 1-2.

^{235}U

R_{If} (0.15 eV - 30 keV) = 283.2 ± 8.5 barn;
R_{If} (1.8 eV - 30 keV) = 175.2 ± 5.3 barn;
R_{Ic} (1.8 eV - 30 keV) = 134.2 ± 8.1 barn;
$\langle\alpha\rangle = 0.766 \pm 0.069$

^{239}Pu

R_{If} (5 eV - 20 keV) = 148.1 ± 4.5 barn;
R_{Ic} (5 eV - 20 keV) = 105.3 ± 9.5 barn;
$\langle\alpha\rangle = 0.711 \pm 0.085$

(see pp. 62-69)

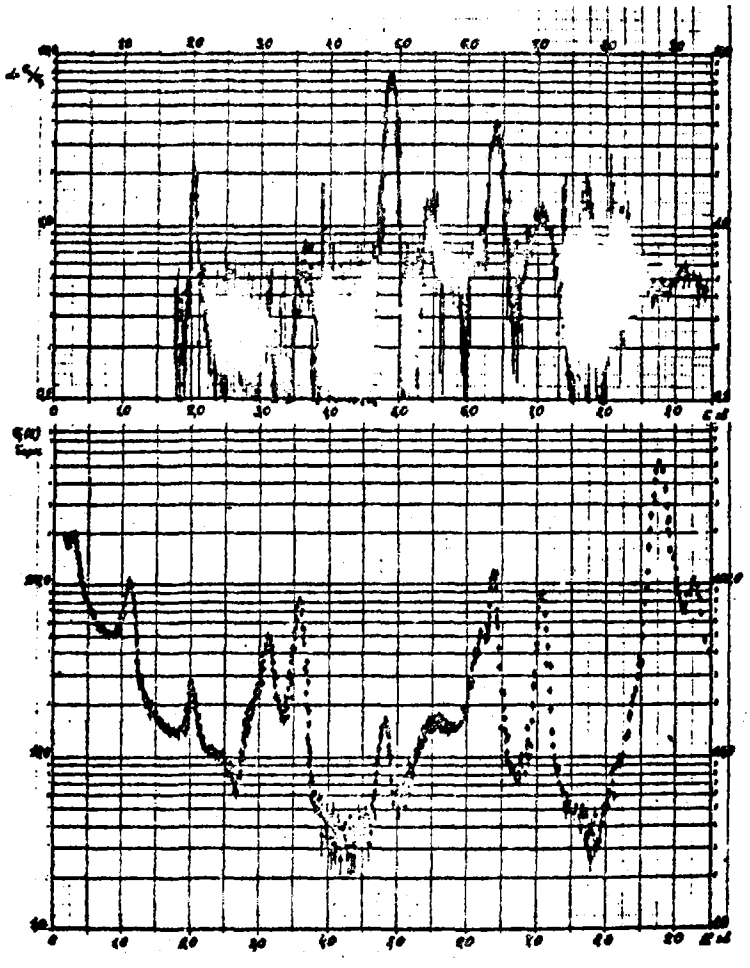

0.2 eV - 10 eV

Fig. 1:

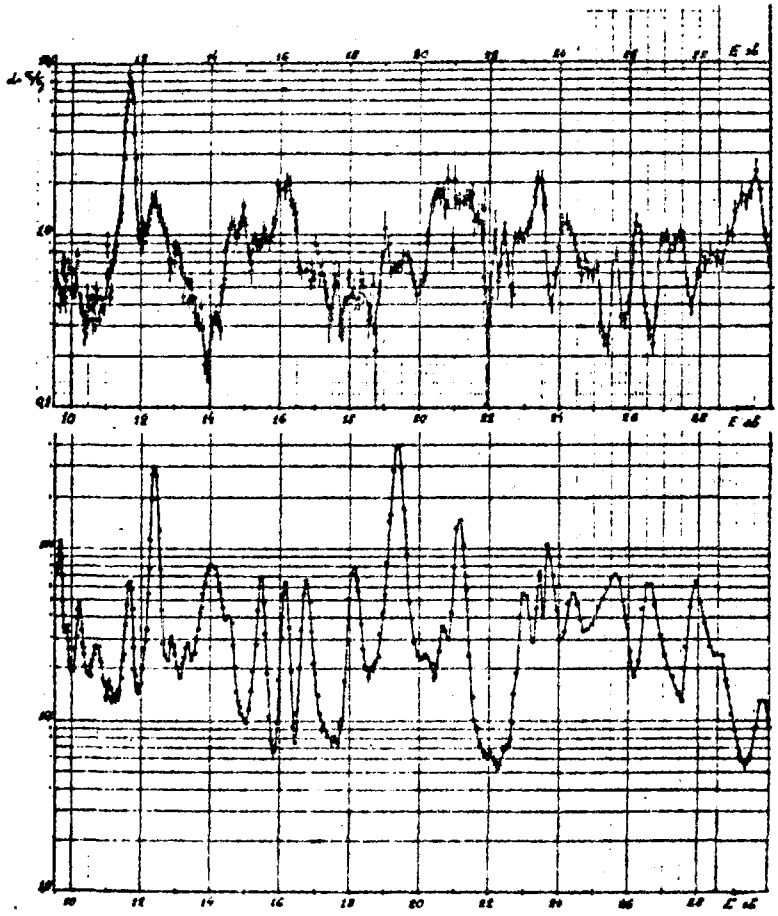

Fig. 2:

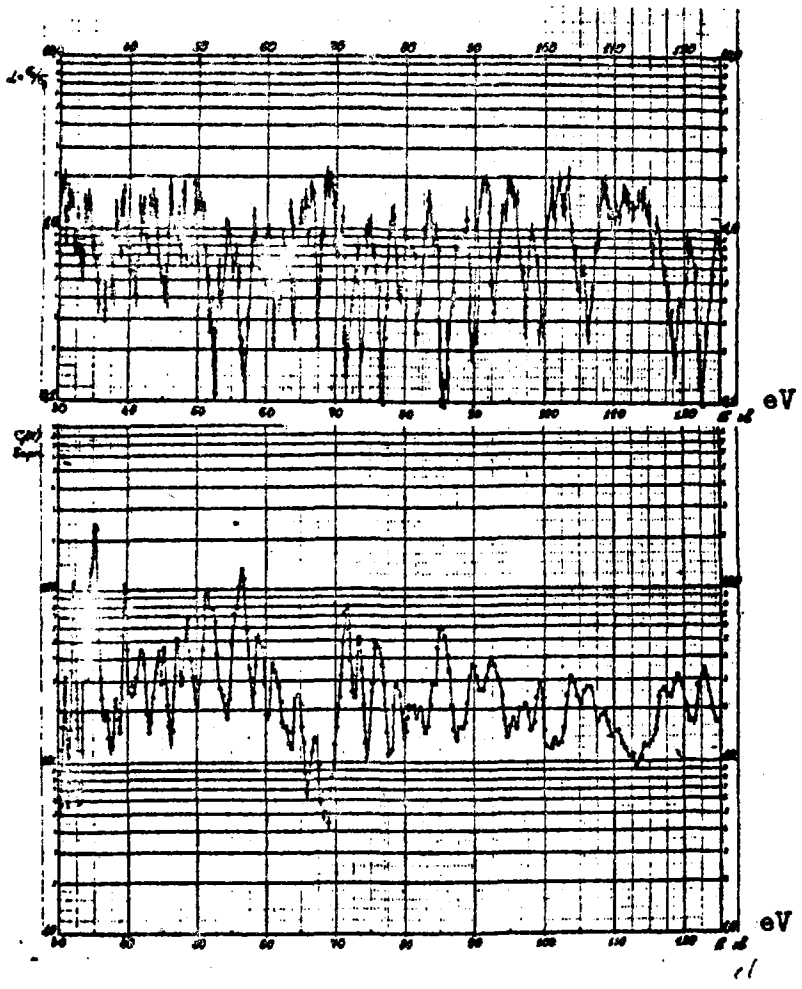

Fig. 3:

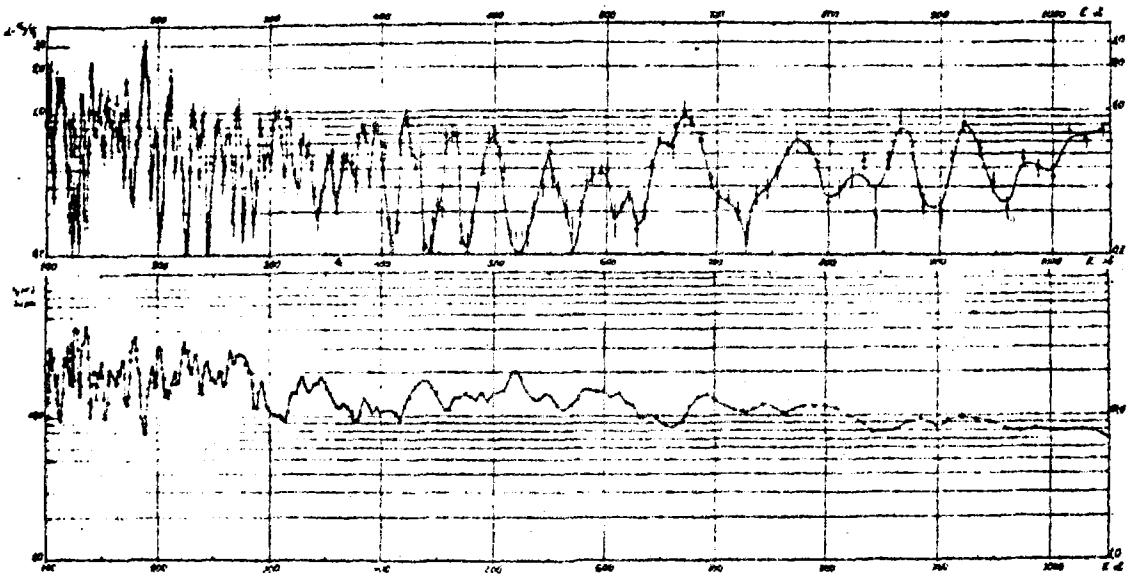

Fig. 4:

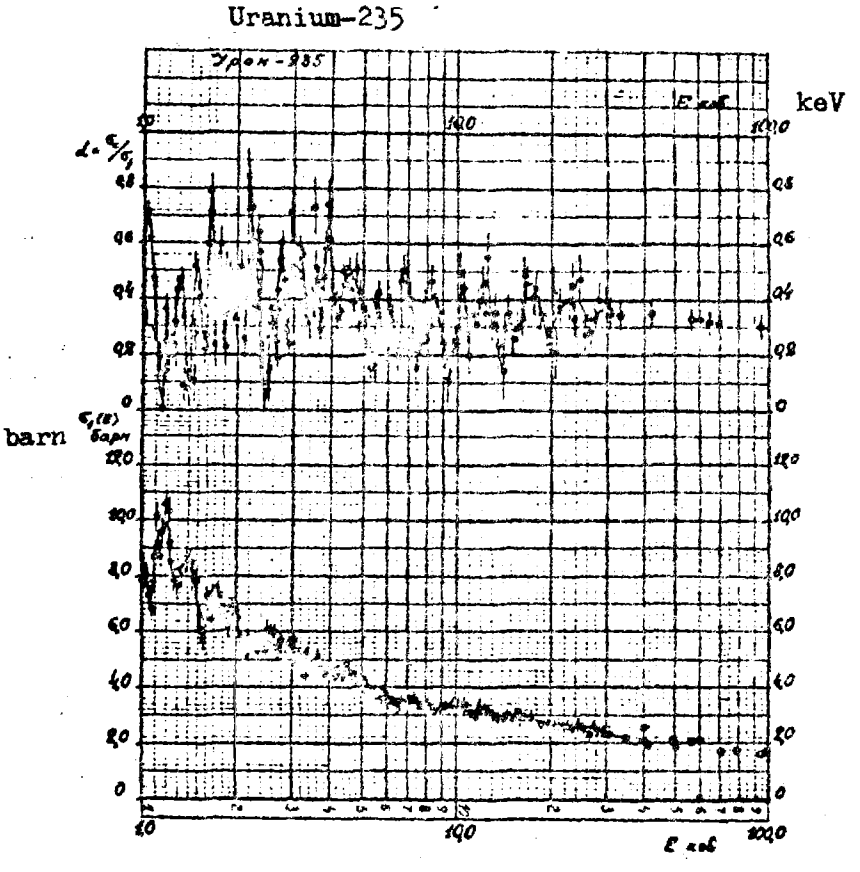

Fig. 5:

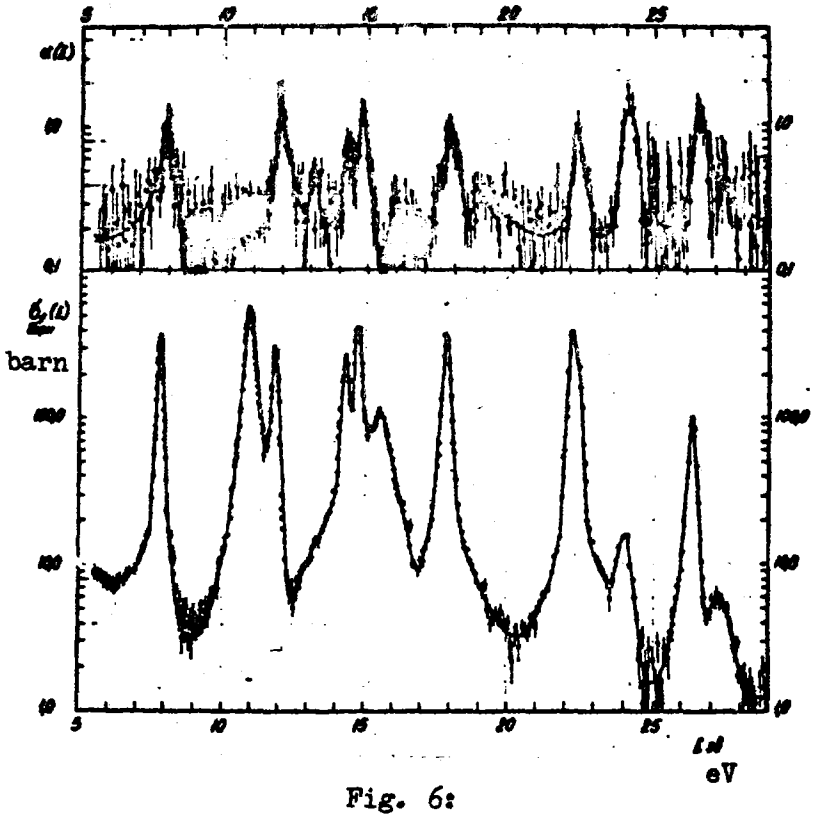

Fig. 6:

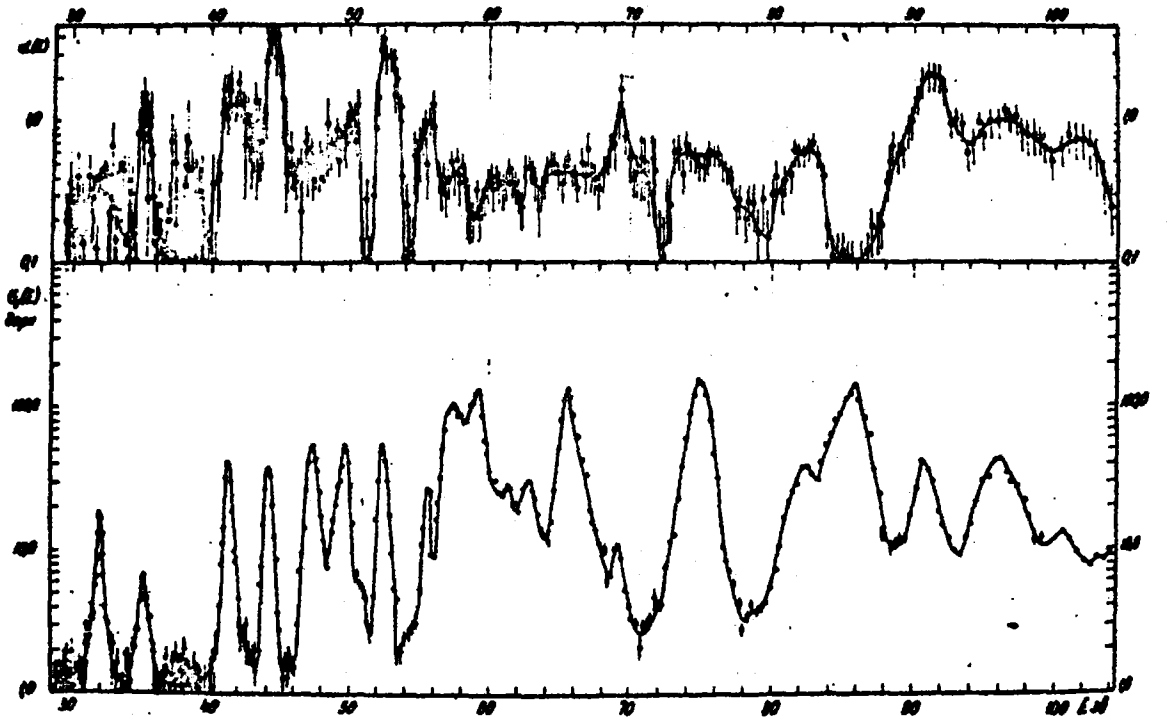

Fig. 7:

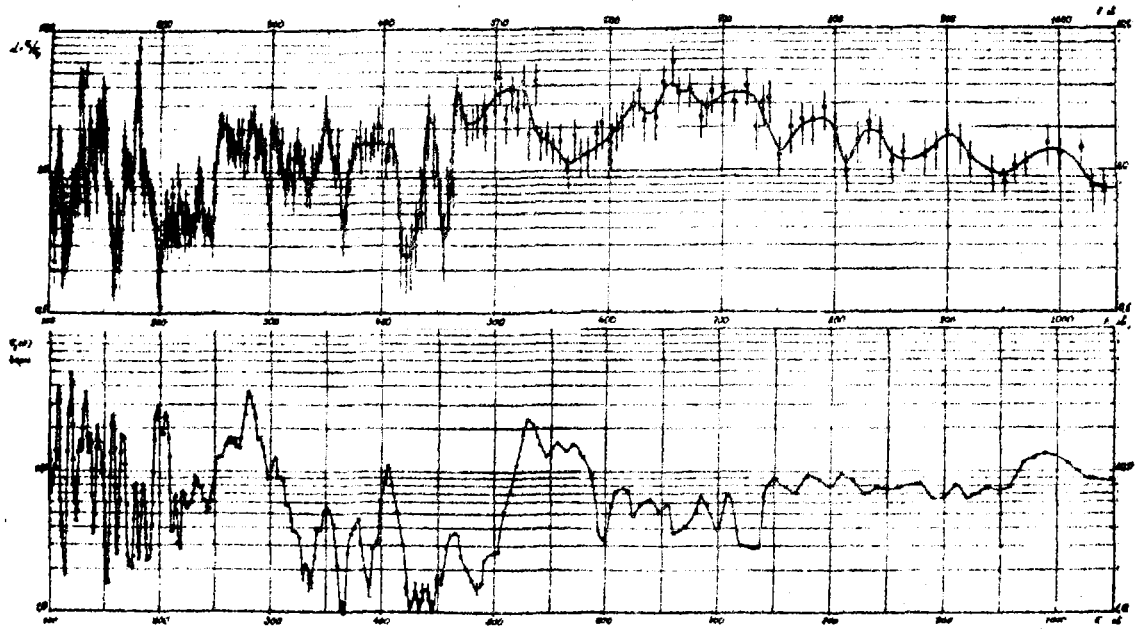

Fig. 8:

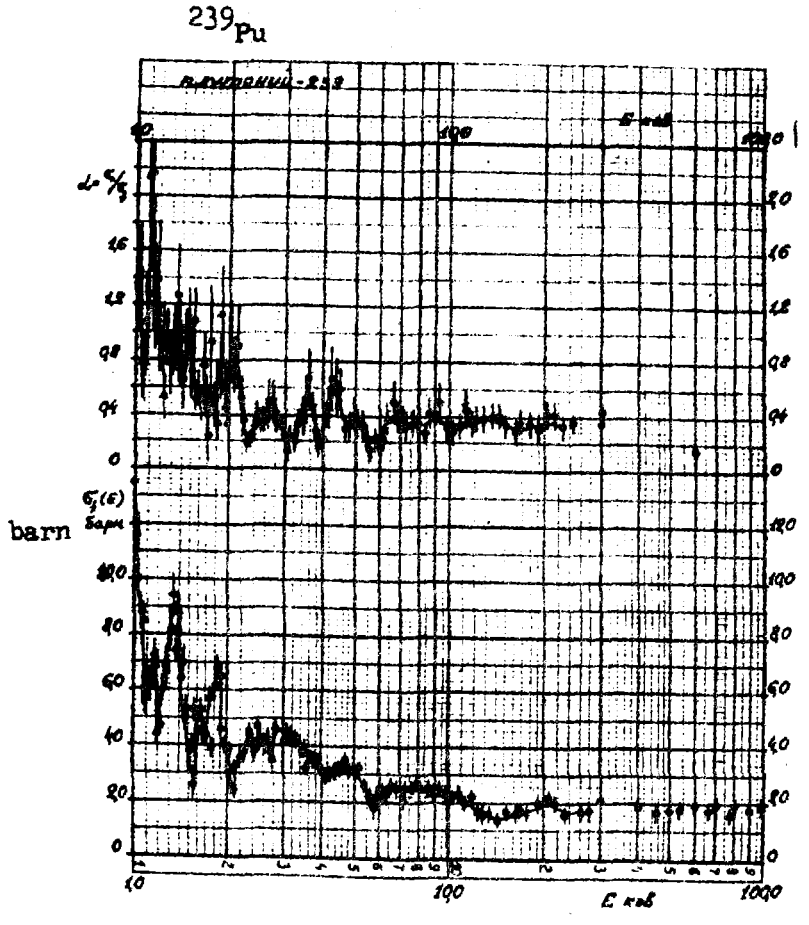

Fig. 9:

Table 1. Resonance integrals of ^{235}U fission and radiative capture*

E (eV)	RI_f		RI_c		
	1	2	3		$\langle\alpha\rangle$
0,15					
0,35	145,1				
0,45	28,6	28,2			
0,50	8,8	8,6			
0,55	6,9	7,2			
0,70	15,0	14,8			
1,0	19,6	19,2			
1,3	18,0	17,4			
1,8	5,6	5,5	5,8		
4,5	16,0	14,9	16,6	7,1	0,43
5,0	0,88	0,84	0,88	3,2	3,64
7,4	8,9	8,2	9,7	14,1	1,45
10,0			21,9	10,4	0,48
15,0			16,4	21,0	1,28
20,5			15,2	11,6	0,76
33,0			16,4	16,0	0,98
41,0			12,7	10,2	0,80
60,0			15,8	11,2	0,71
73,0			4,4	2,9	0,66
100,0			8,1	5,2	0,64
113,0			2,1	2,3	1,10
200,0			12,0	8,7	0,73
300,0			8,4	4,5	0,54
1000,0			14,6	5,8	0,40
3000,0			7,6	2,8	0,37
10000,0			4,8	1,8	0,38
20000,0			2,1	0,73	0,35
30000,0			0,94	0,33	0,35

*Remarks: 1. Measurements with gas scintillation counter.

2. Measurements with ionization fission chamber.

3. Measurements with liquid scintillation detector.

Table 2. Resonance integrals of ^{239}Pu fission and radiative capture*

E (эв)	RI_f	RI_c	$\langle\alpha\rangle$
5,0			
7,4	2,6	0,67	0,27
I0,0	I2,6	9,I	0,72
I5,0	46,4	25,3	0,55
20,5	I4,9	6,7	0,45
33,0	I0,9	6,4	0,59
4I,0	0,43	0,I3	0,30
60,0	9,9	9,5	0,96
73,0	5,7	2,5	0,44
I00,0	II,8	6,2	0,53
II3,0	I,6	I,7	I,06
200,0	7,5	8,6	I,I5
300,0	5,4	6,8	I,26
I000,0	7,8	I5,4	I,97
3000,0	5,8	4,6	0,79
I0000,0	3,55	I,27	0,36
20000,0	I,25	0,43	0,35

*Measurements with liquid scintillation detector.